

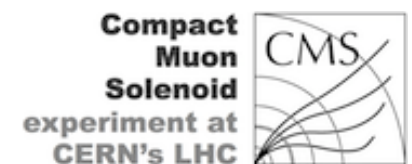
Higgs boson properties

(ATLAS and CMS)

Marcello Fanti [University of Milano and INFN]

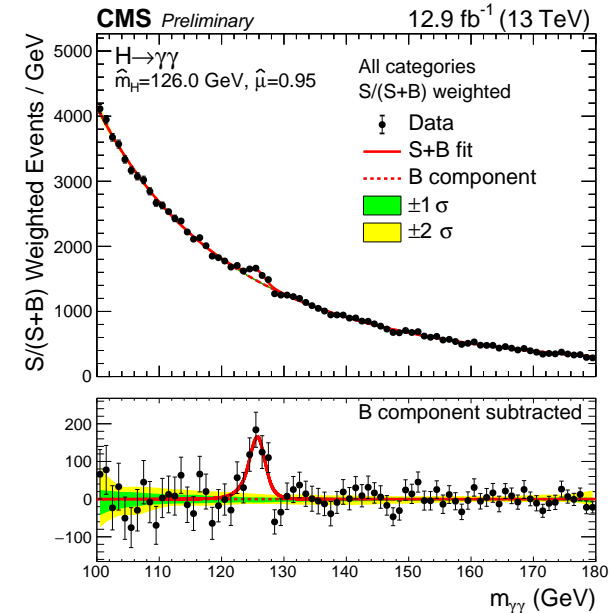
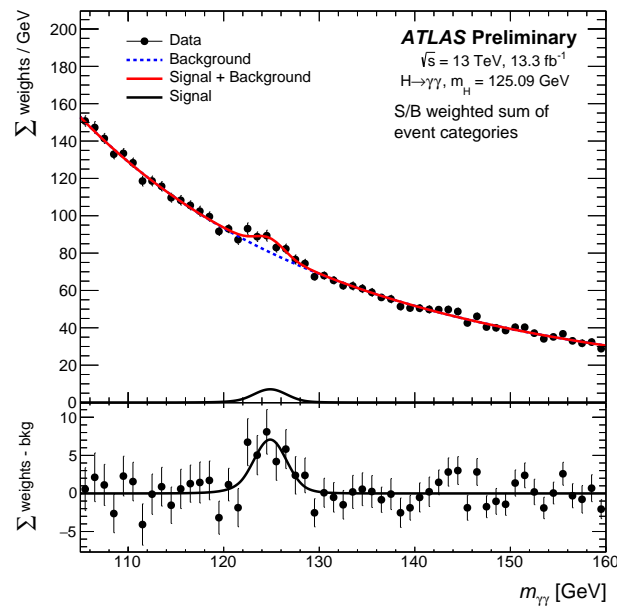


(on behalf of the ATLAS and CMS collaborations)

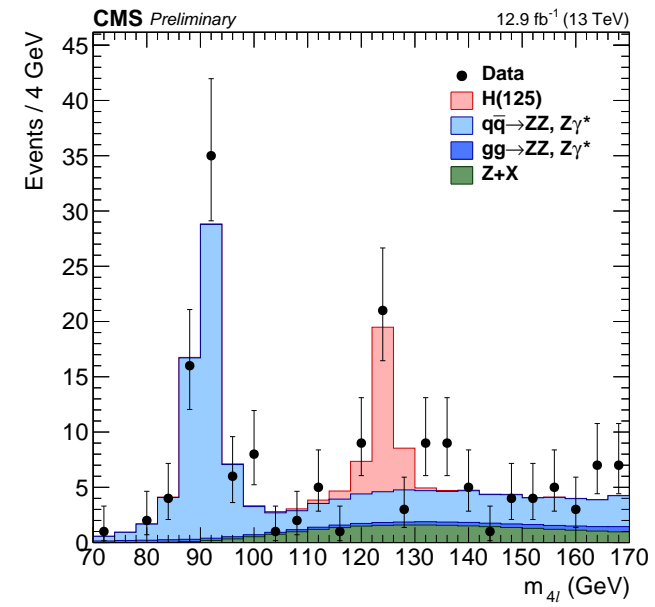
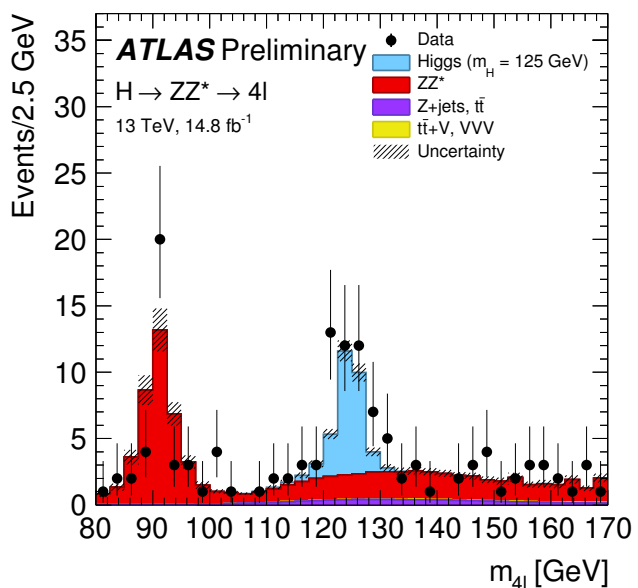


Run-II : Higgs boson strikes back!

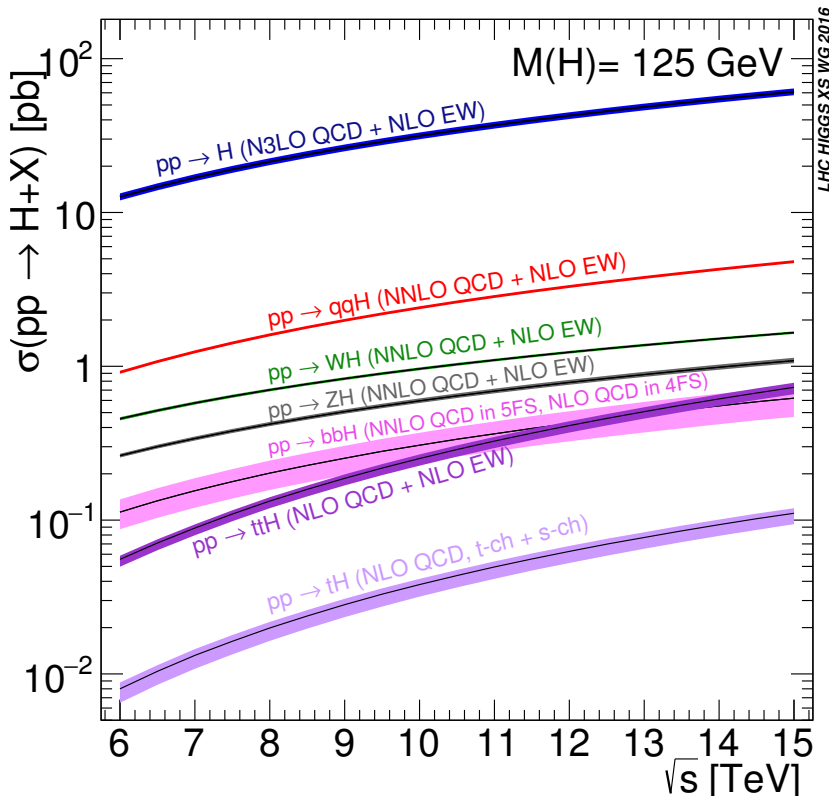
$H \rightarrow \gamma\gamma$



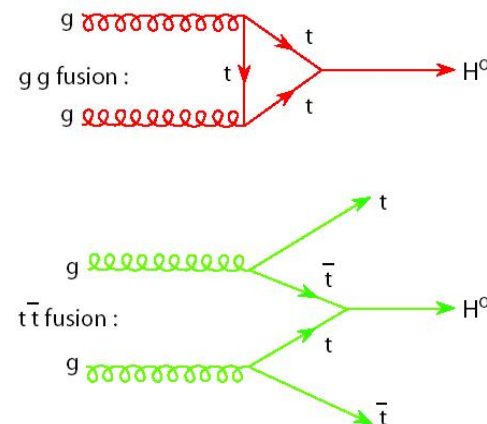
$H \rightarrow 4l$



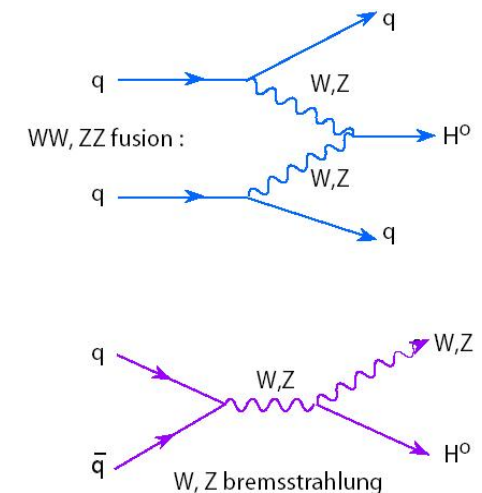
Higgs boson production at LHC



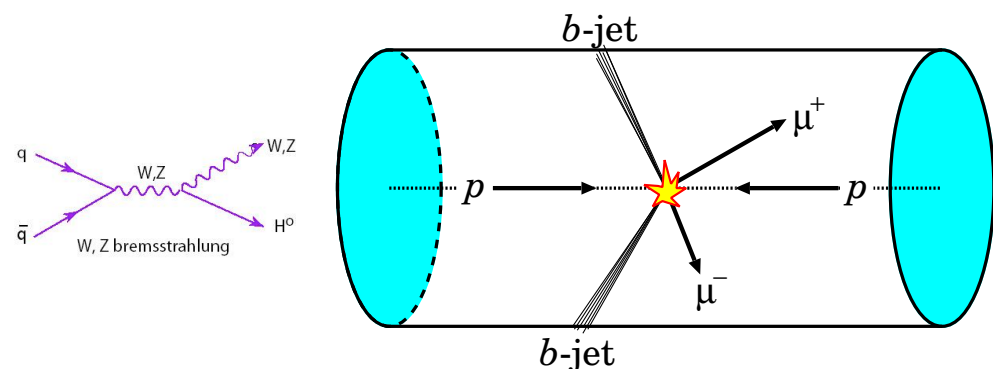
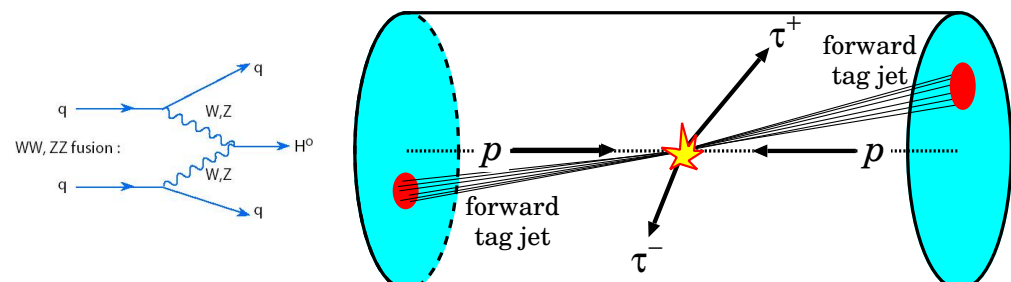
QCD production



EW production



Experimental identification of VBF and VH productions (“tagging”):



Higgs at LHC : Run-I vs Run-II

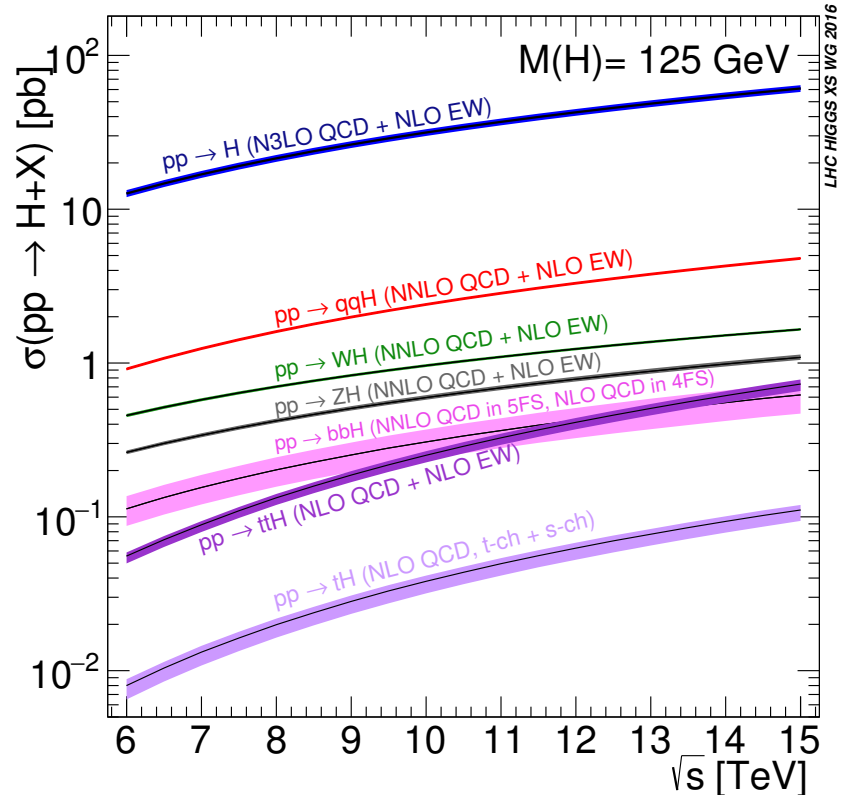
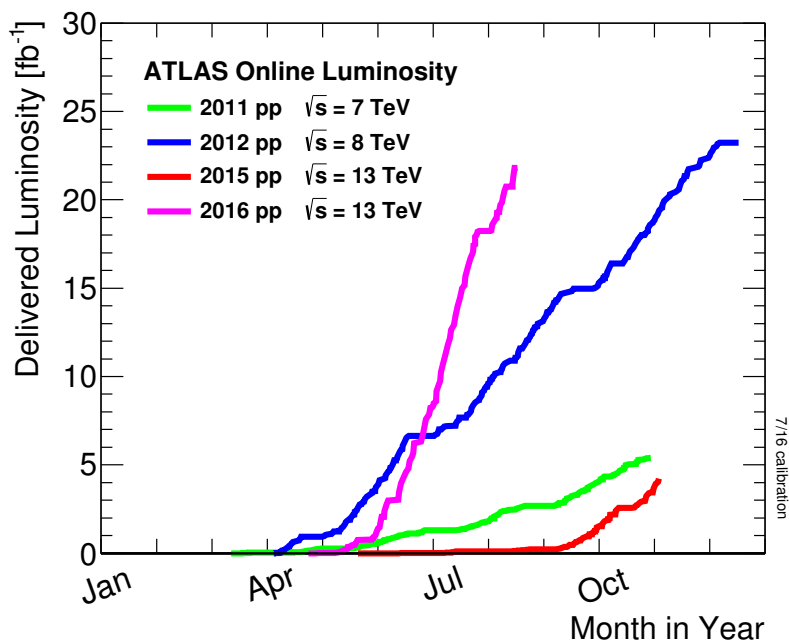
Cross-section vs \sqrt{s}

$$\sqrt{s} = 8 \text{ TeV} \longrightarrow 13 \text{ TeV}$$

cross-sections increase:

ggF, VBF by $2.3 \times$

ttH by $3.8 \times$



Luminosity per experiment

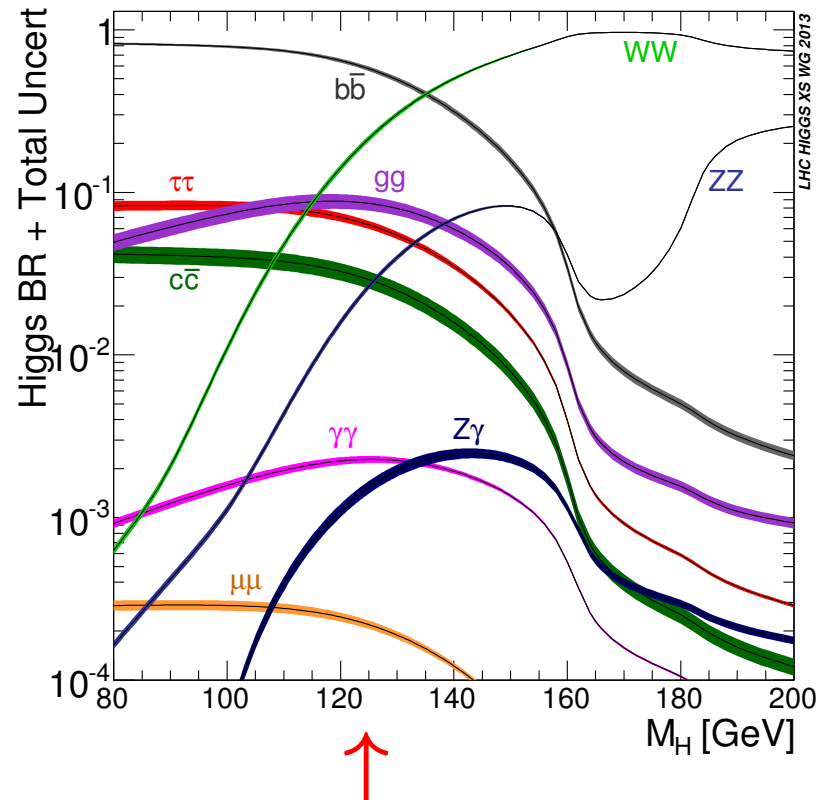
In Run-I $\Rightarrow \approx 25 \text{ fb}^{-1}$

In 2015 $\Rightarrow \approx 3 \text{ fb}^{-1}$

In 2016 $\Rightarrow \approx 21 \text{ fb}^{-1}$ and rising fast!
($\approx 9 - 15 \text{ fb}^{-1}$ analysed)

Higgs boson decay modes

For a mass $m_H \simeq 125 \text{ GeV}$, several decay modes are kinematically accessible
⇒ a thorough study of its properties is possible



If it is the Standard Model Higgs boson, its properties are:

- spin-parity : $J^{CP} = 0^{++}$
- couplings to vector bosons : $g_V = 2 \frac{m_V^2}{v}$
- couplings to fermions : $g_f = \frac{m_f}{v}$

⇒ can probe several couplings and J^{CP} states

Observation of $H \rightarrow \gamma\gamma \Rightarrow C = +1$ and $J \neq 1$ (Landau-Yang theorem)

Higgs at LHC : Run-I vs Run-II

Mass measurement

From run-I, combined ATLAS+CMS measurement
Now repeated at Run-II

Cross-sections, Couplings

Fiducial and total cross-sections at 7, 8, 13 TeV
Couplings from run-I combined ATLAS+CMS measurement, and being repeated in Run-II
ttH production and $H \rightarrow b\bar{b}$

Spin and CP properties, width, differential cross-sections

From Run-I, being repeated in Run-II

Mass measurement

[arXiv:1503.07589v1 [hep-ex] 26 Mar 2015 PRL 114 (2015) 191803]

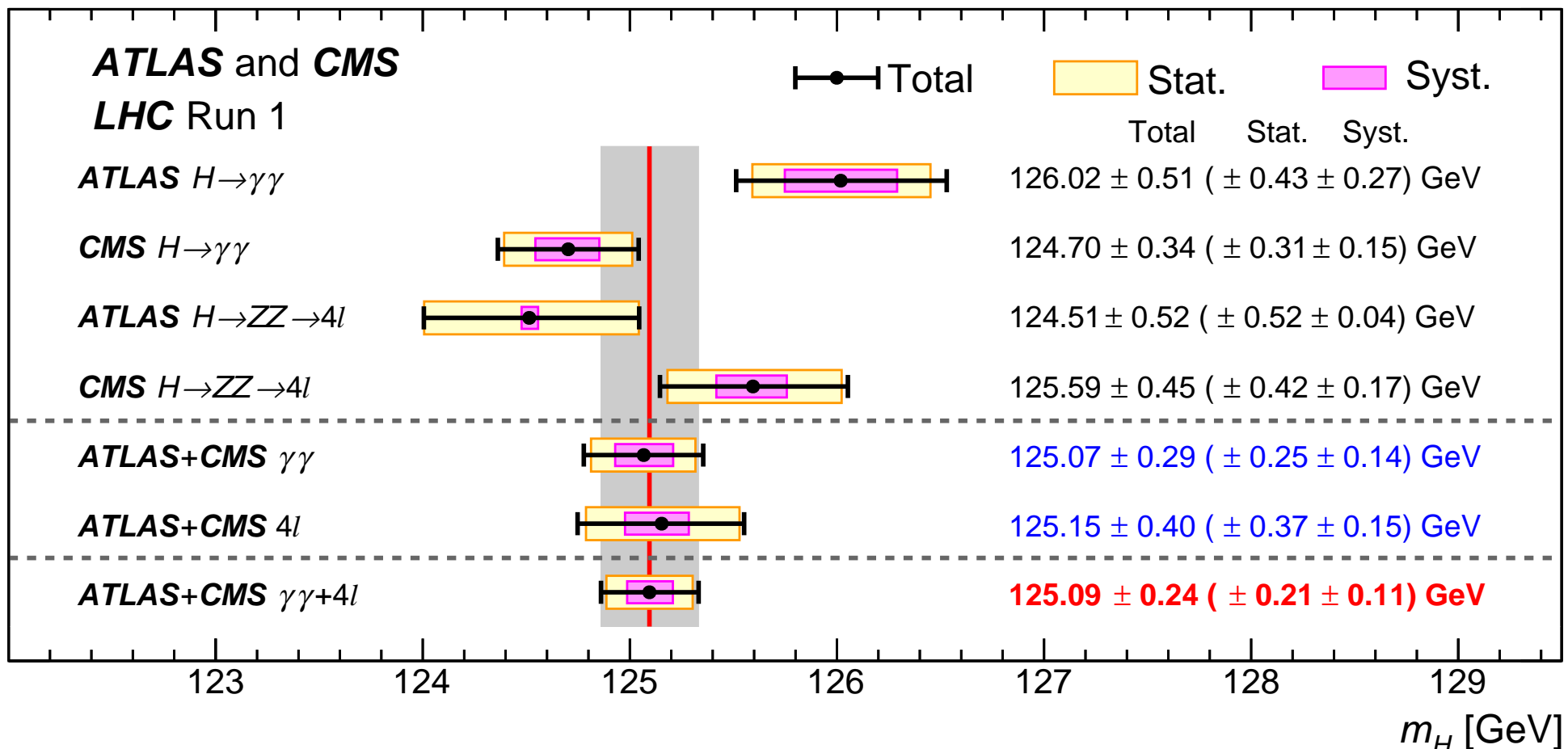
Mass measurement

Using the

$H \rightarrow \gamma\gamma$ and $H \rightarrow ZZ^* \rightarrow 4l$ decay channels

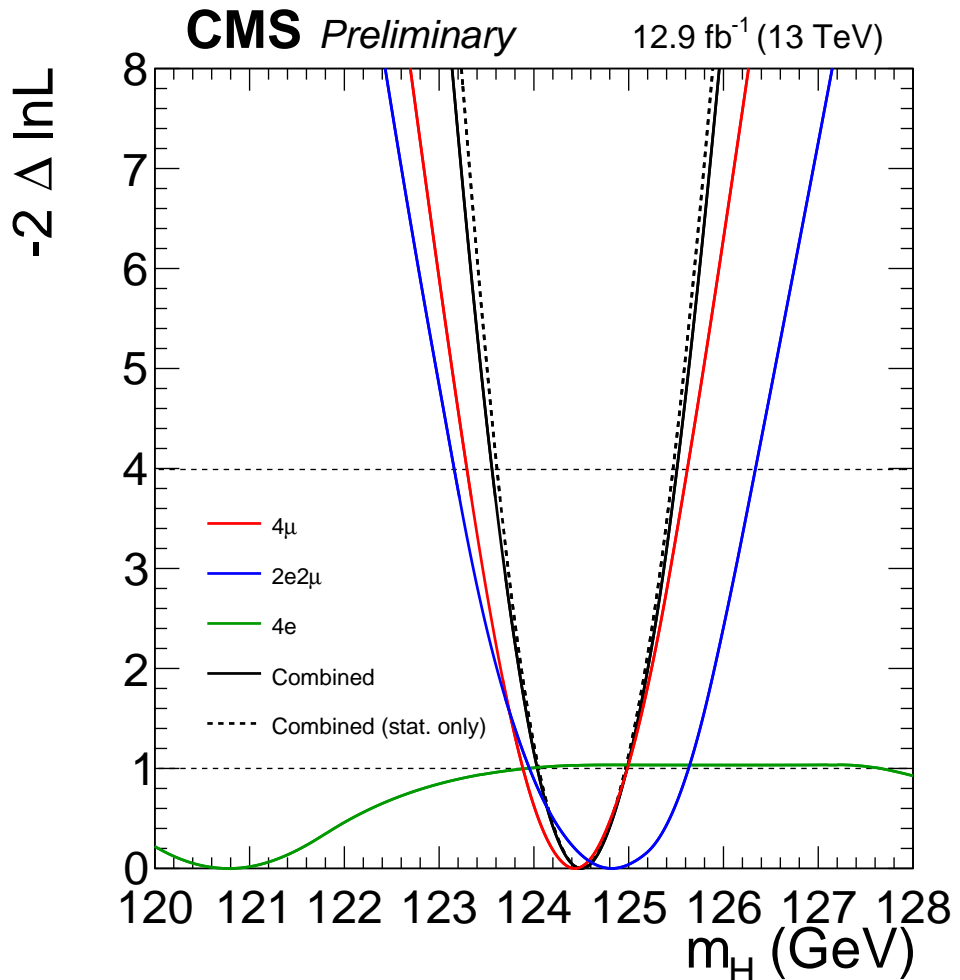
that allow a full kinematics reconstruction with good invariant mass resolution ($\mathcal{O}(1 \text{ GeV})$)

(main source of systematic: energy scale)



$$\hat{m}_H = 125.09 \pm 0.21(stat) \pm 0.11(syst) \text{ GeV}$$

Mass measurement @ 13 TeV



CMS , $H \rightarrow 4\ell$ channel

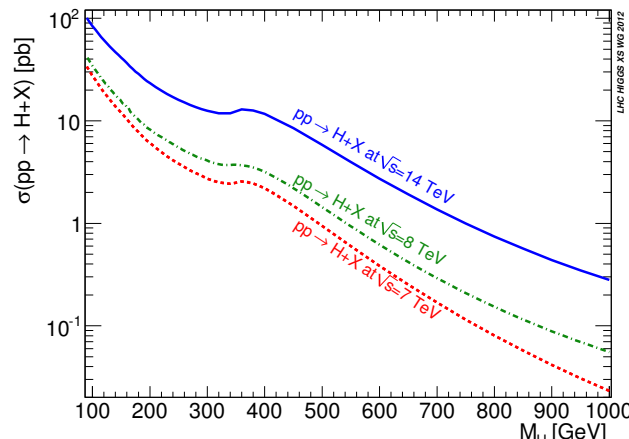
$$\hat{m}_H = 124.50^{+0.47}_{-0.45}(\text{stat})^{+0.13}_{-0.15}(\text{syst}) \text{ GeV}$$

Importance of mass measurement

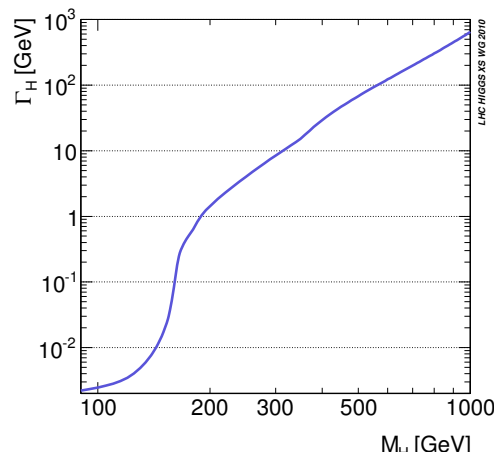
In the Standard Model, m_H is the only free parameter of the Higgs sector

The Higgs sector has two parameters: μ and λ related to the VEV v and the Higgs mass m_H by: $\mu = \frac{m_H}{\sqrt{2}}$ and $\lambda = \frac{1}{2} \left(\frac{m_H}{v} \right)^2$. Since $v = \sqrt{\frac{1}{\sqrt{2} G_F}}$ is known, m_H is the only free parameter.

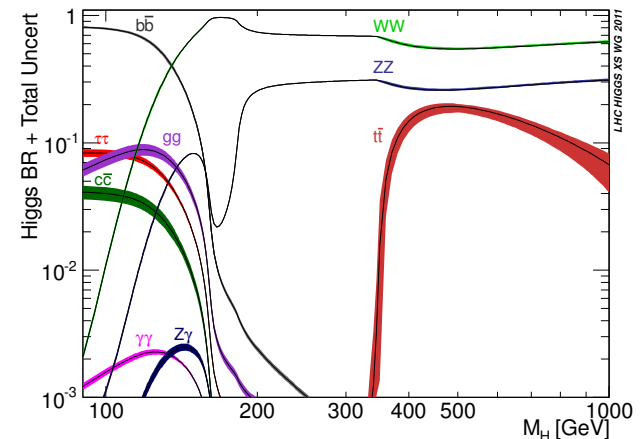
cross-section



decay width



branching ratios



⇒ everything else is calculable, once m_H is given.

[<https://twiki.cern.ch/twiki/bin/view/LHCPhysics/CERNYellowReportPageBR>]

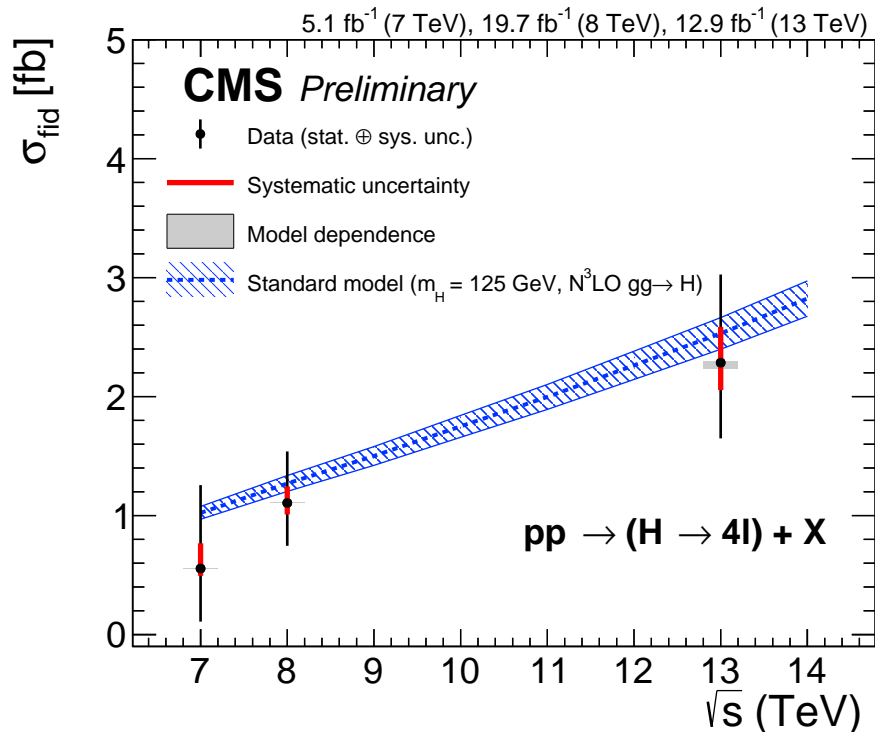
Cross sections

Cross-section from $\gamma\gamma$ and 4ℓ final states

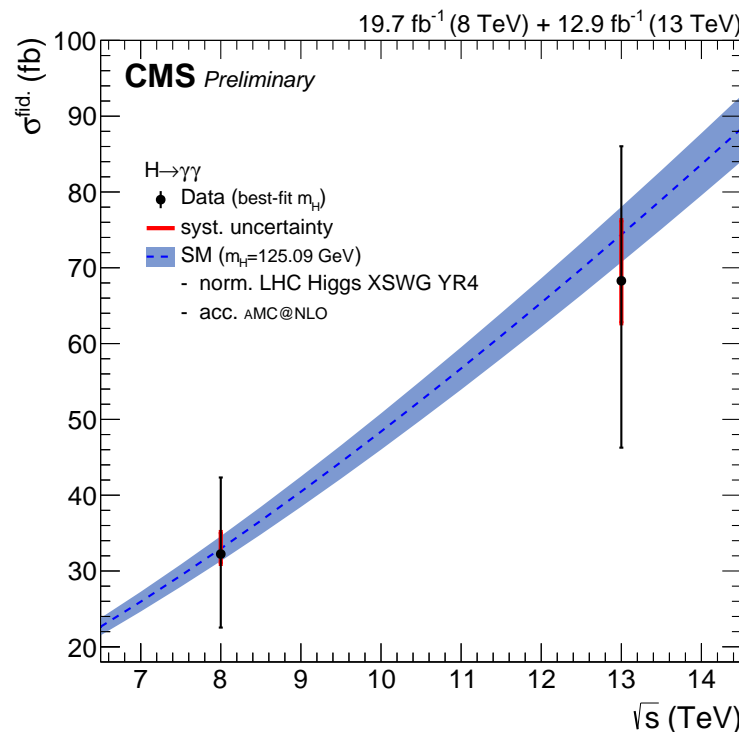
[CMS-PAS-HIG-16-033 , CMS-PAS-HIG-16-020]

Fiducial cross-section vs \sqrt{s}

$H \rightarrow 4\ell$



$H \rightarrow \gamma\gamma$



Improved theory calculations for gluon fusion:

Run-I: NNLO+NNLL: $\pm 8\%$ from scale and $\pm 7\%$ from α_S +PDF

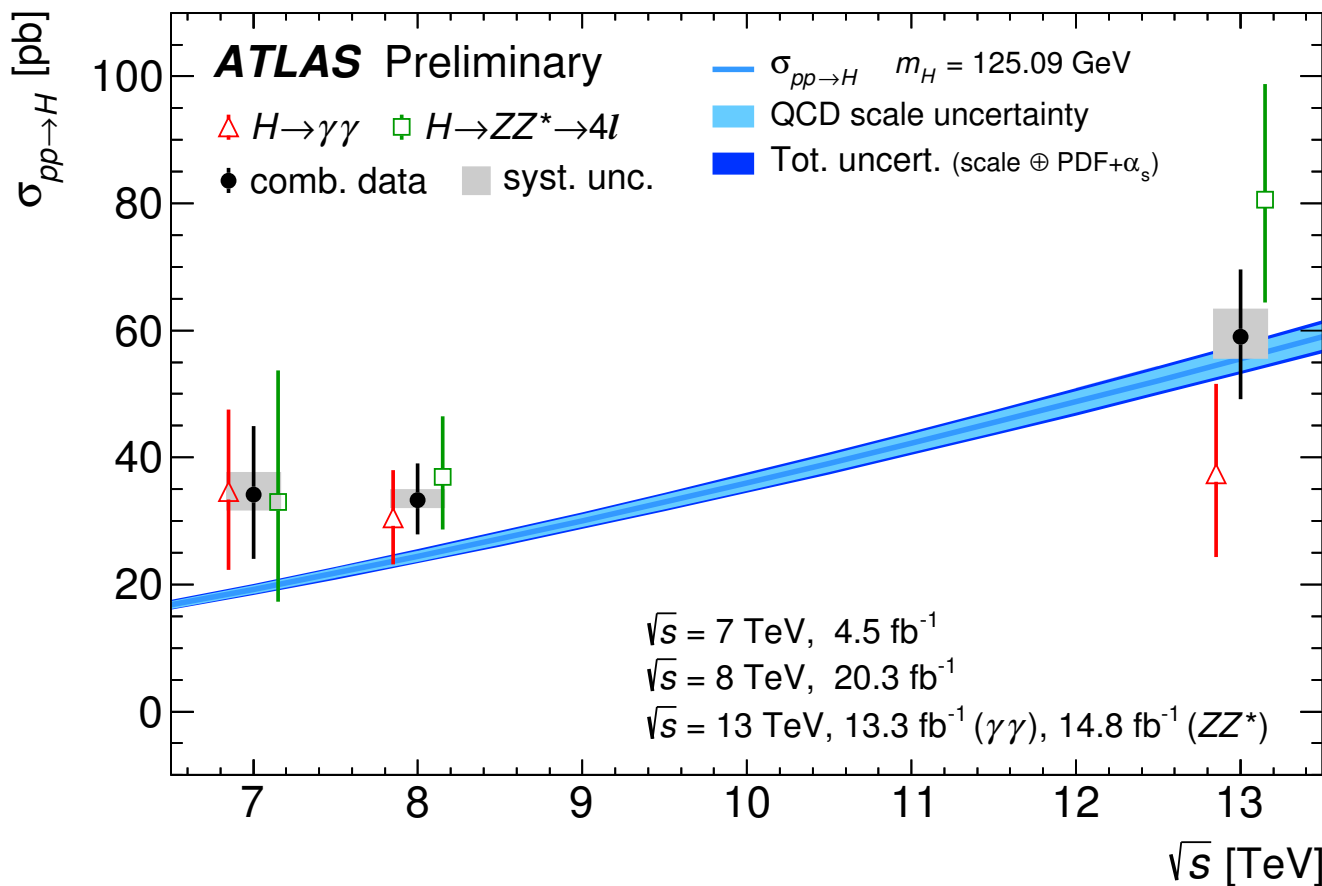
Run-II: N3LO: $\pm 4\%$ from scale and $\pm 3\%$ from α_S +PDF

... now experiments need to catch up!

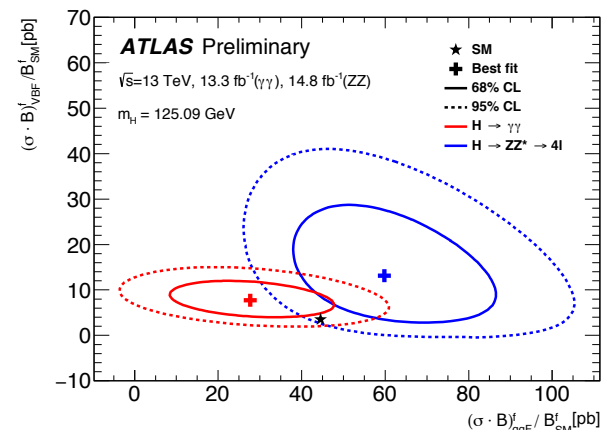
Cross-section from $\gamma\gamma$ and 4ℓ final states

[ATLAS-CONF-2016-081]

Total cross-section vs \sqrt{s} ($\gamma\gamma$ and 4ℓ combined)



Cross-section for ggF vs VBF



Measurements of couplings

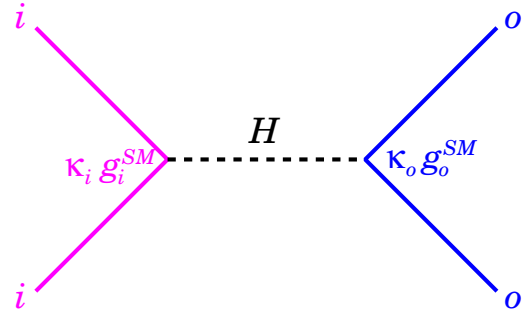
[arXiv:1606.02266v1 [hep-ex] 7 Jun 2016 accepted by JHEP]

Couplings — the “ κ -framework”

Reminder: in SM Higgs couplings are $g_f^{SM} = \frac{m_f}{v}$ and $g_V^{SM} = 2\frac{m_V^2}{v}$

Couplings are accessible through production ($ii \rightarrow H$) and decay ($H \rightarrow oo$)

Define “couplings modifiers” $\kappa_x = \frac{g_x}{g_x^{SM}}$



$$\Rightarrow \sigma_{ii \rightarrow H \rightarrow oo} = \sigma_{ii \rightarrow H \rightarrow oo}^{SM} \times \frac{\kappa_i^2 \kappa_o^2}{\kappa_H^2}$$

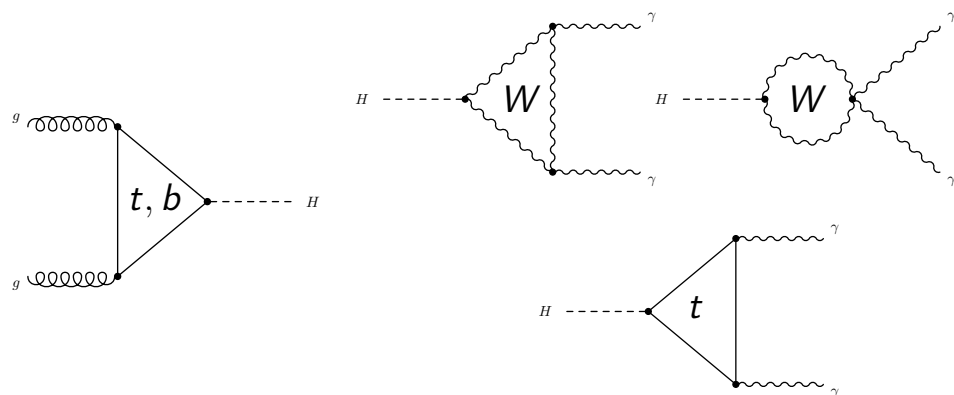
$$(\kappa_H^2 \stackrel{\text{def}}{=} \frac{\Gamma_H}{\Gamma_H^{SM}} \text{ — if no BSM decays, } \kappa_H^2 = \sum_o \kappa_o^2 BR_{H \rightarrow oo}^{SM})$$

(... otherwise need to allow one extra free parameter, BR to new physics, BR_{BSM} — see later on)

\Rightarrow Several couplings: $\kappa_\mu, \kappa_\tau, \kappa_b, \kappa_W, \kappa_Z, \kappa_t \dots$

\Rightarrow effective couplings: $\kappa_g, \kappa_\gamma \dots$

Assume weak gauge boson universality: $\kappa_W = \kappa_Z = \kappa_V$ and fermion universality: $\kappa_t = \kappa_b = \kappa_\tau = \kappa_f$



Loop-mediated interactions described as in SM:

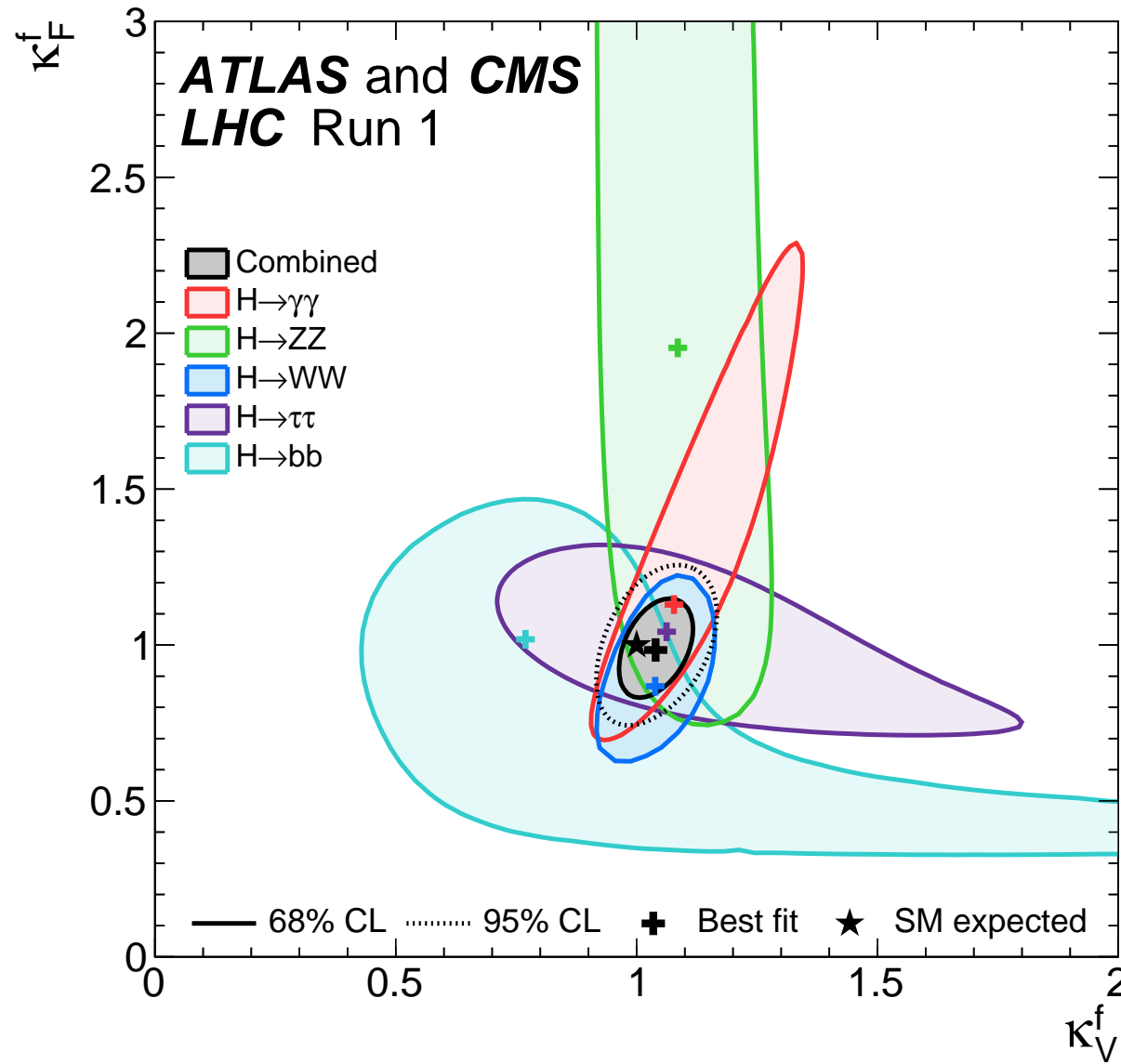
$gg \rightarrow H$ (mainly) through top/bottom virtual loop

$$\Rightarrow \kappa_g = \kappa_{t,b} = \kappa_f$$

$H \rightarrow \gamma\gamma$ through top and W virtual loops

$$\Rightarrow \kappa_\gamma^2 = (1.26 \kappa_W - 0.26 \kappa_t)^2 = (1.26 \kappa_V - 0.26 \kappa_f)^2$$

(Universal) couplings to fermions and weak bosons



Exploit final state topologies (e.g.
VBF, VH)

⇒ measure κ_V , κ_f for each decay channel

⇒ then combine decay channels

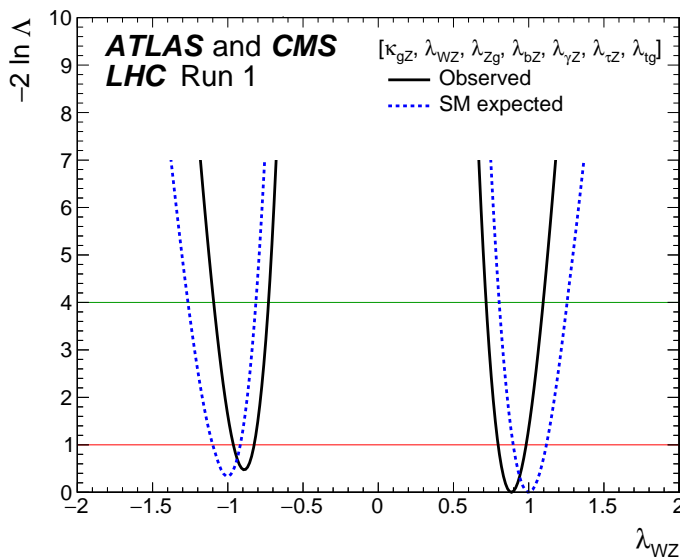
⇒ all measurements compatible
with SM prediction (★)

$$(\kappa_V = 1, \kappa_f = 1)$$

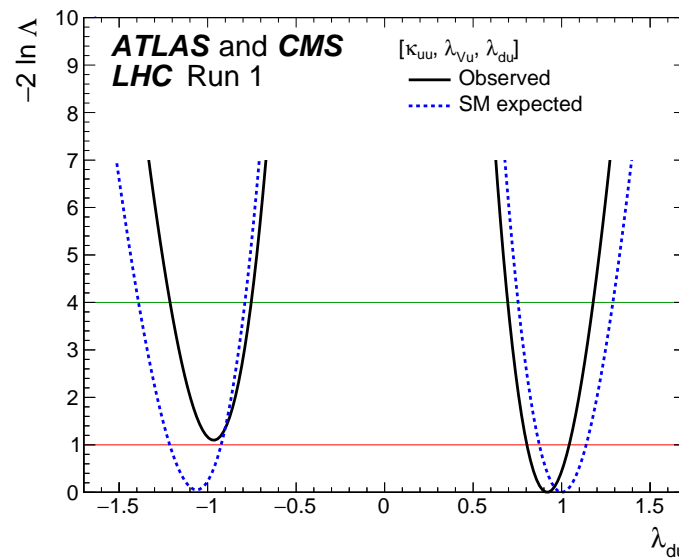
Relaxing some assumptions

Testing the EW symmetry breaking:

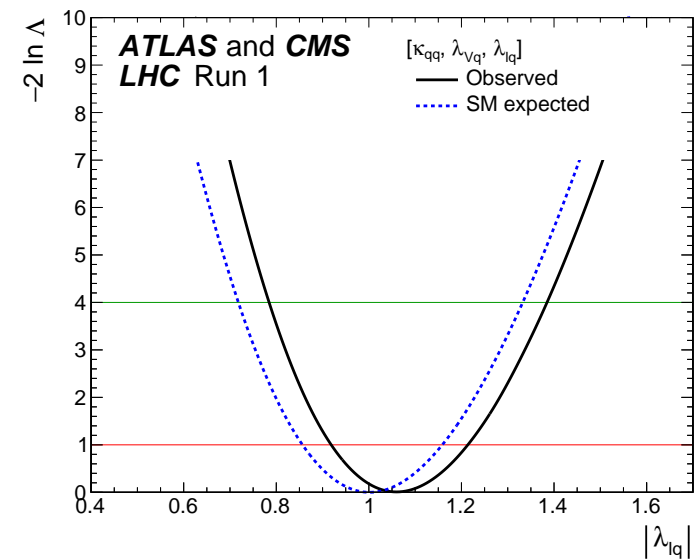
$$\lambda_{WZ} = \frac{\kappa_W}{\kappa_Z}$$



$$\lambda_{du} = \frac{\kappa_d}{\kappa_u}$$

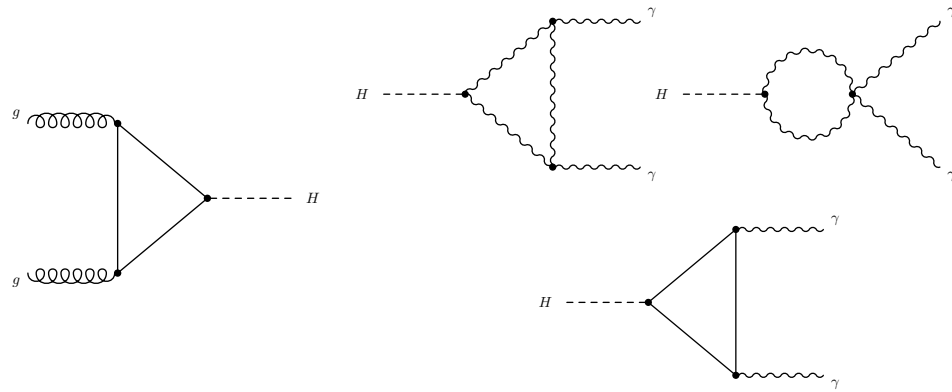


$$\lambda_{\ell q} = \frac{\kappa_\ell}{\kappa_q}$$

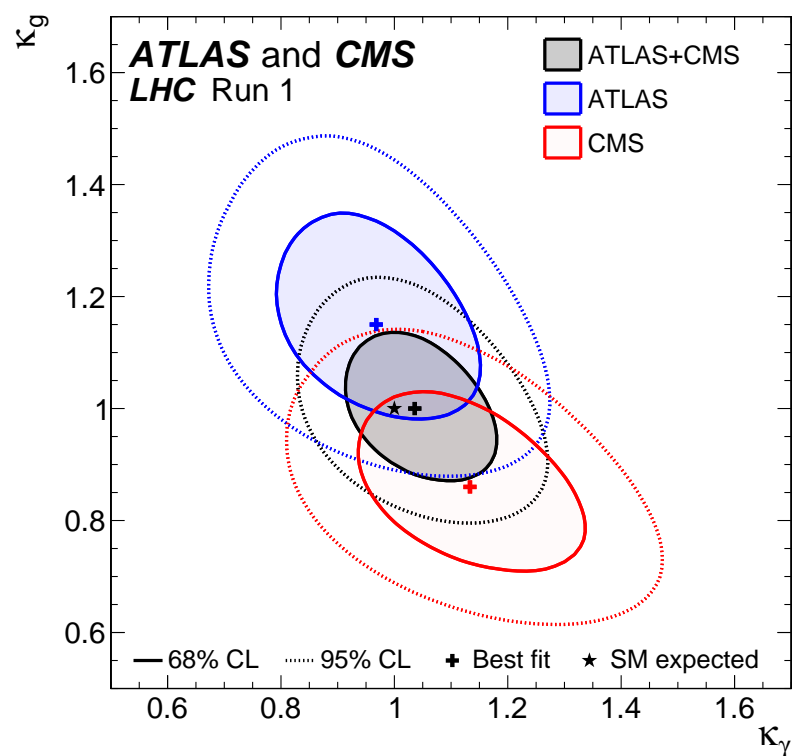


Testing up/down and lepton/quark universality
(would be broken in 2-Higgs-doublet models)

Testing the ggH and H $\gamma\gamma$ interactions

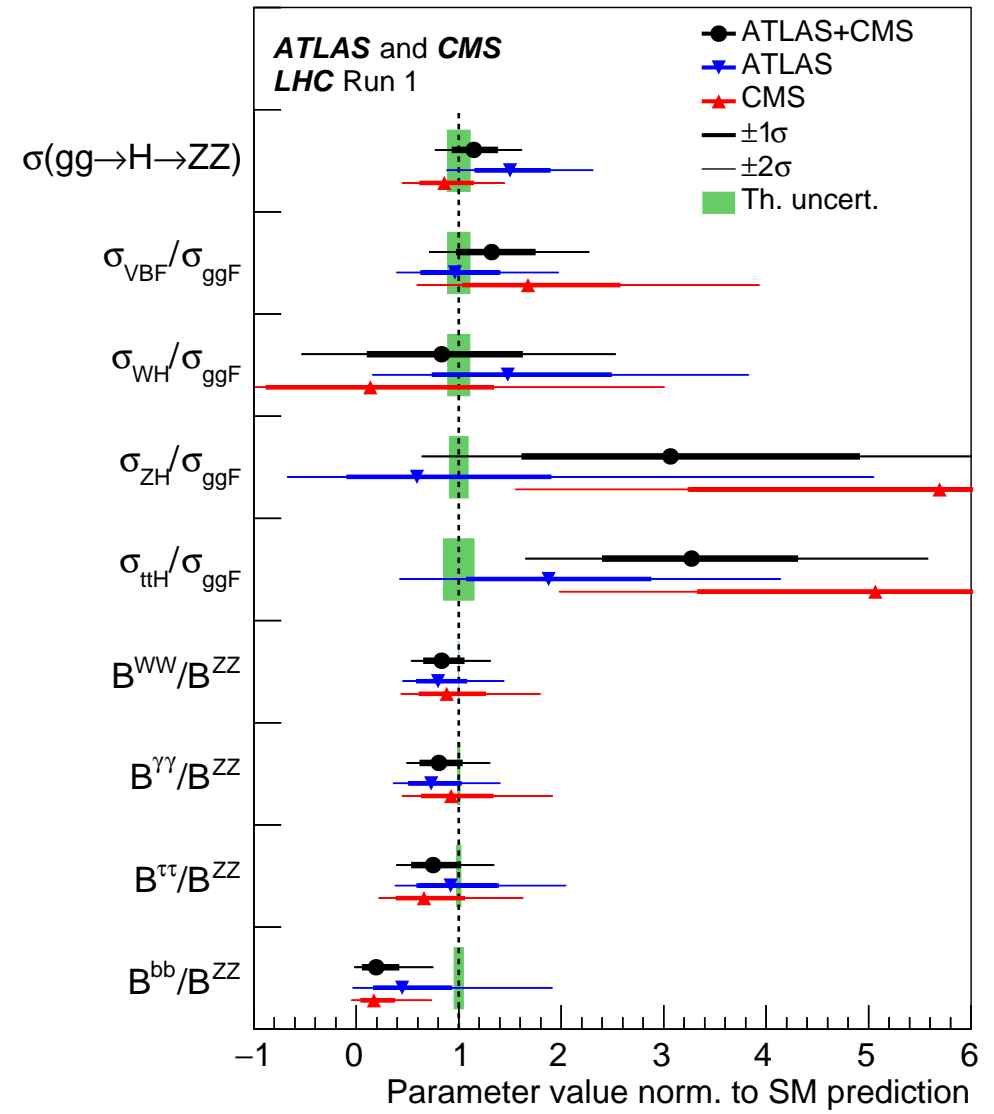
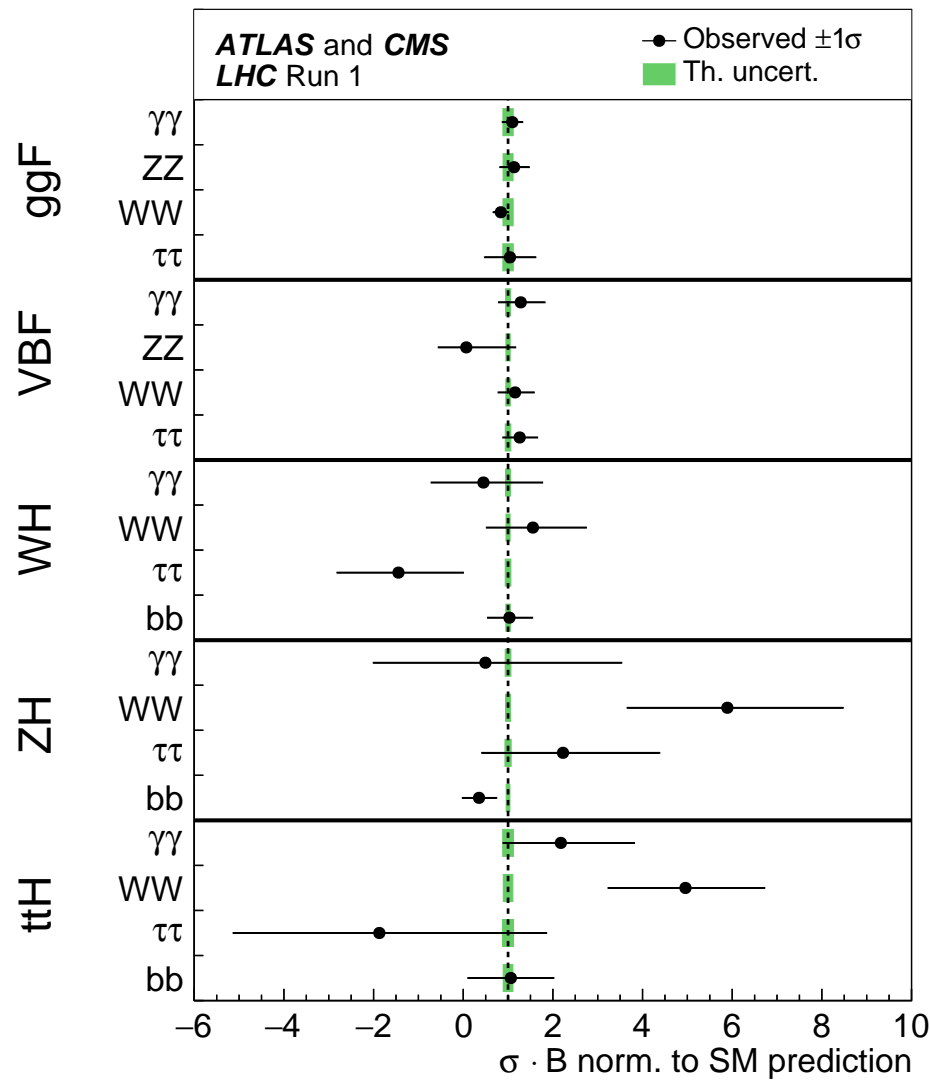


ggH and $H\gamma\gamma$ interactions in SM are mediated by loops
⇒ particularly sensitive to new particles in the loops

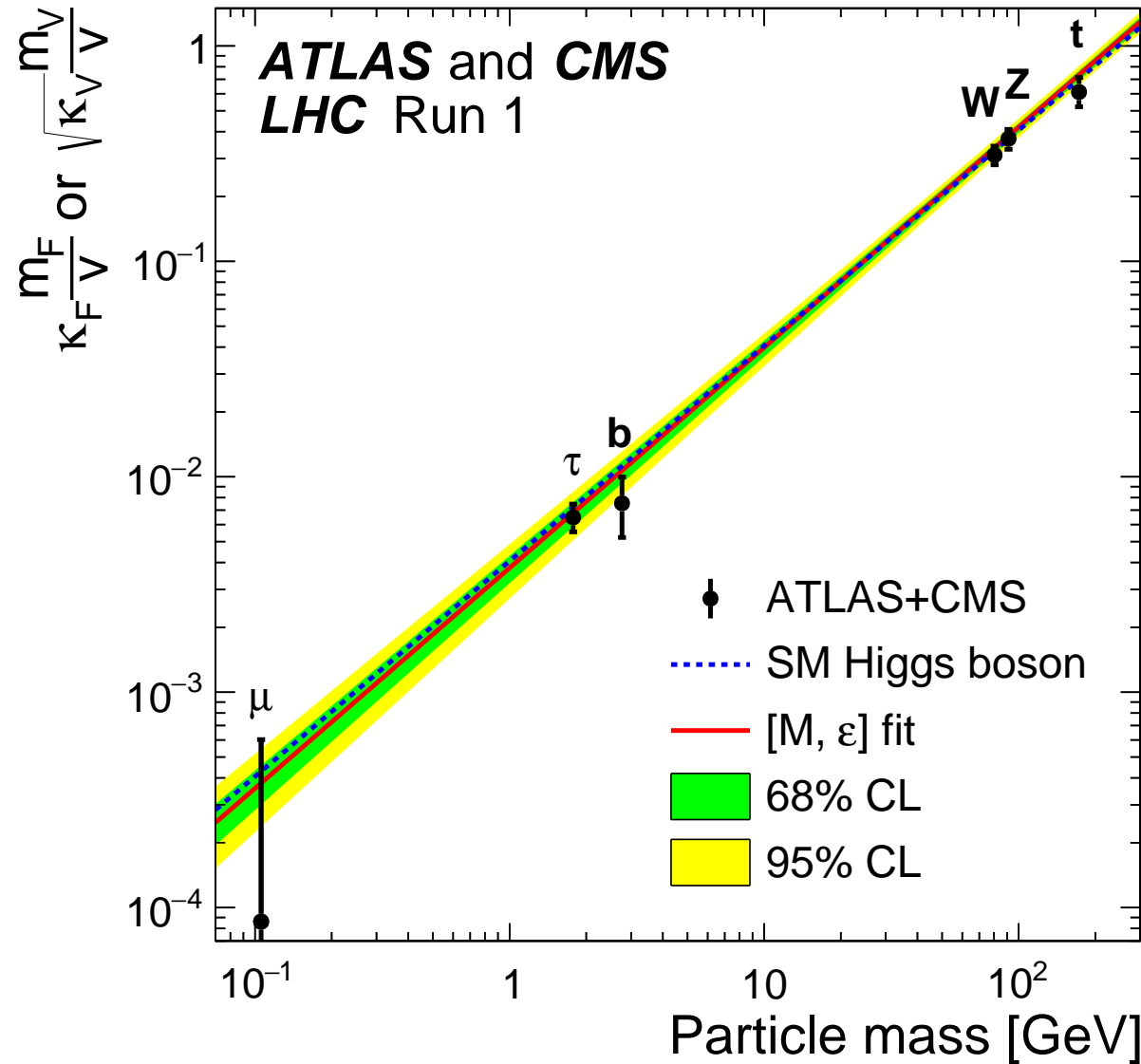


⇒ consider κ_g , κ_γ as free and profile others
⇒ again, compatibility with SM (★)

Summary of the rates (wrt Standard Model predictions)



Summary of the couplings



Recall: in SM

$$g_f = \frac{m_f}{v} \text{ and } g_V = 2 \frac{m_V^2}{v}$$

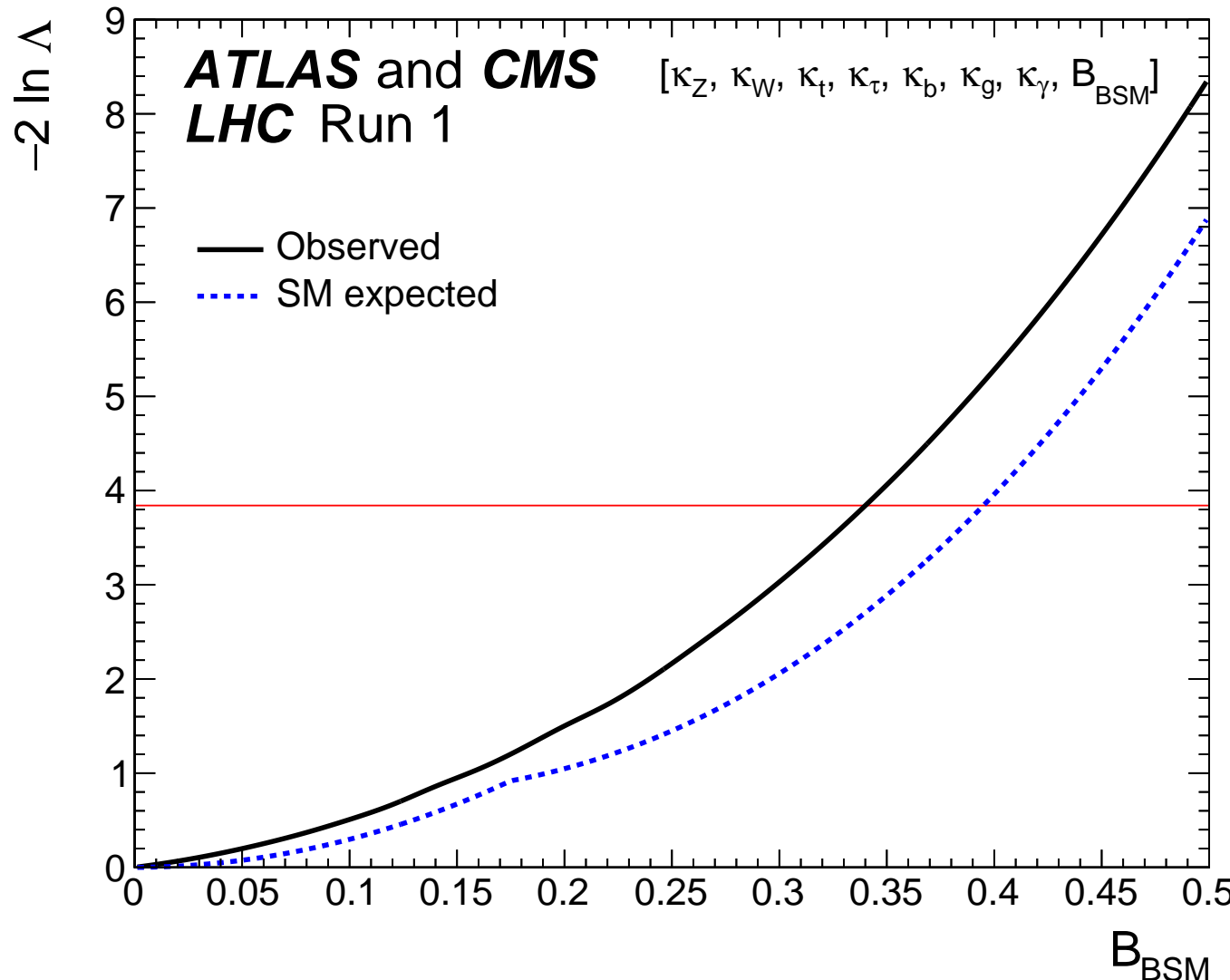
\Rightarrow plot measured g_f vs m_f and

$$\text{measured } \sqrt{\frac{g_V}{2v}} \text{ vs } m_V$$

\Rightarrow all scale like $\frac{m}{v}$ as expected, over more than 3 orders of magnitude!

\Rightarrow Standard Model works pretty well

Testing decays to BSM particles



A branching ratio to BSM particles
 B_{BSM} is allowed as a free parameter

⇒ upper limit at 95% C.L. :

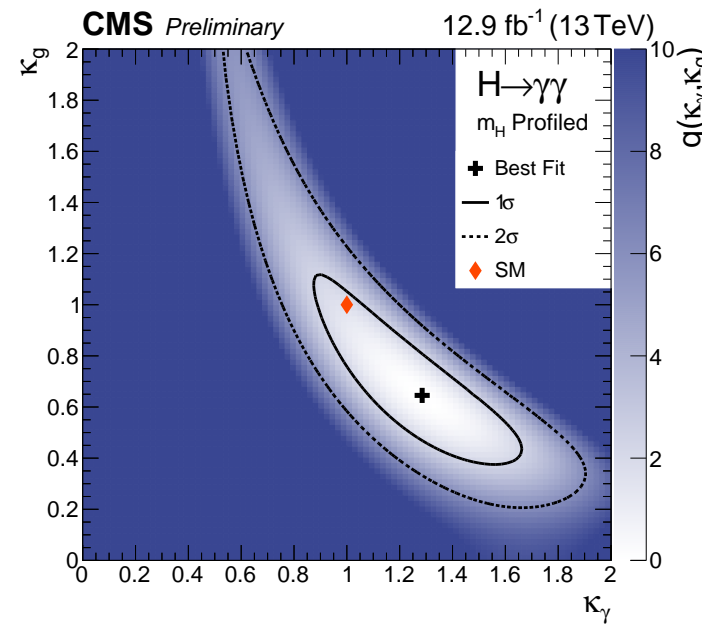
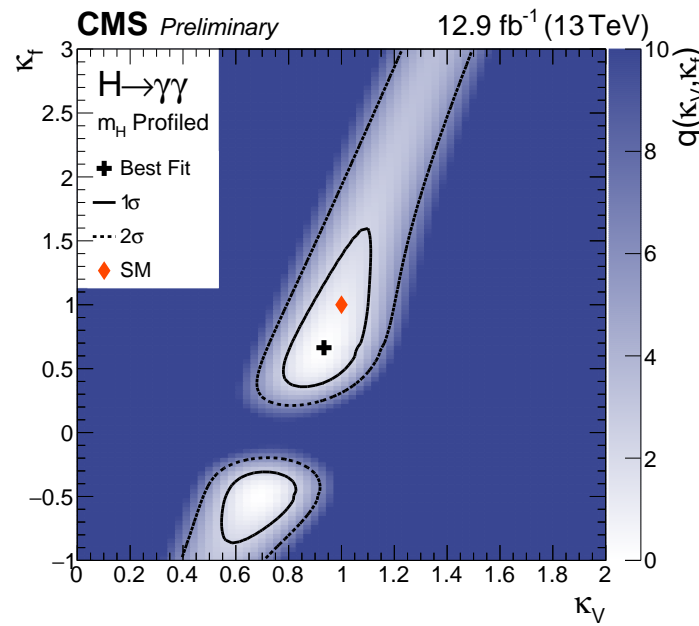
$$B_{BSM} < 0.34$$

(expected: $B_{BSM} < 0.39$)

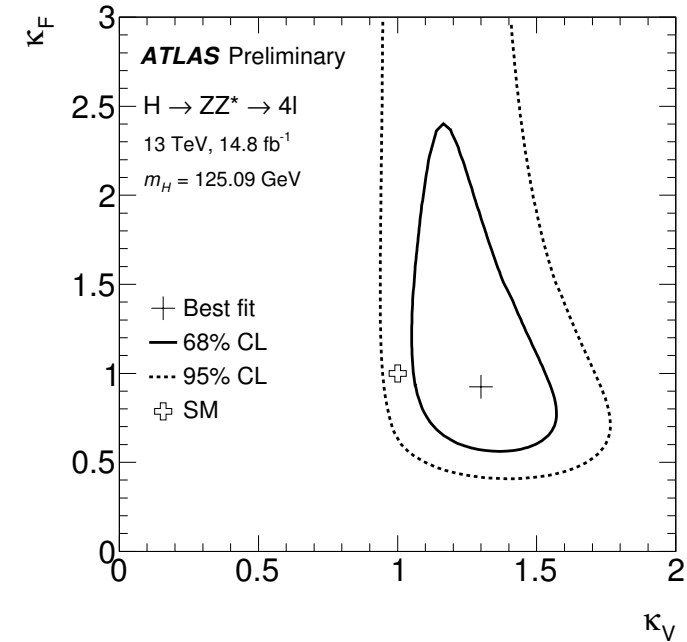
Couplings at 13 TeV

[CMS-PAS-HIG-16-020] , [ATLAS-CONF-2016-079]

$H \rightarrow \gamma\gamma$ channel

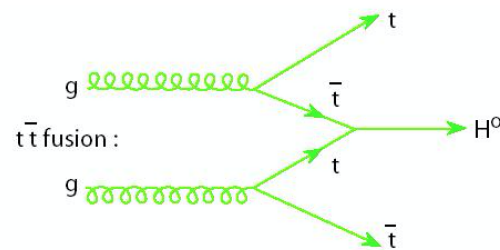


$H \rightarrow 4\ell$ channel



ttH production

[ATLAS-CONF-2016-068 , ATLAS-CONF-2016-080 , ATLAS-CONF-2016-058] , [HIG-16-022]



- important to probe directly the ttH Yukawa coupling
- cross-section 4× higher @ 13 TeV wrt 8 TeV

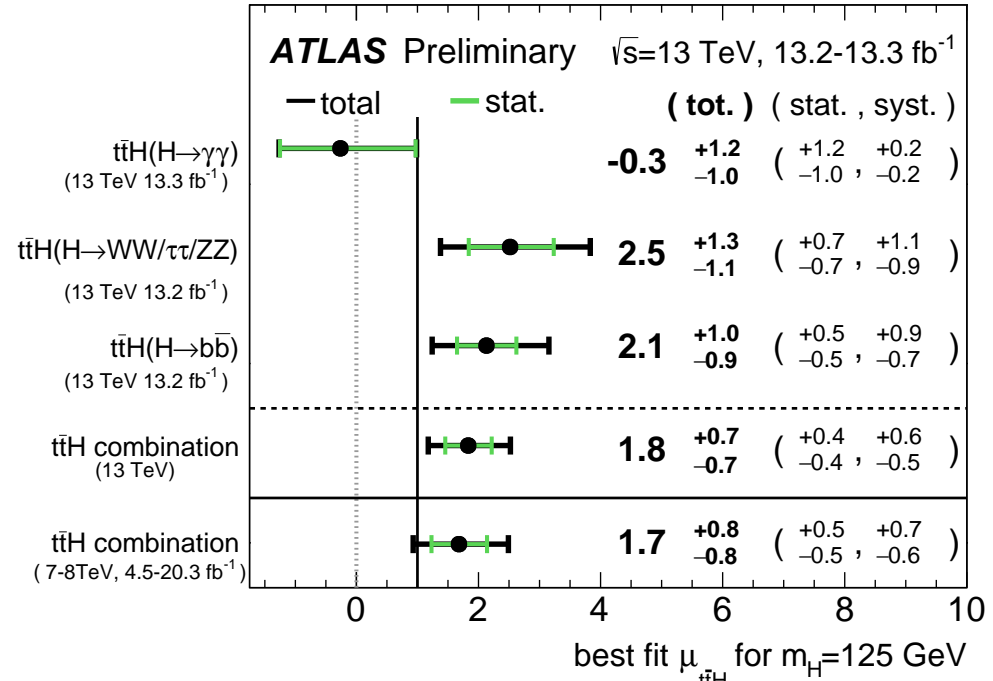


Table 2: Observed and expected asymptotic 95% CL upper limits on and best fit value of the signal strength parameter (μ).

Category	Obs. limit	Exp. limit $\pm 1\sigma$	Best fit $\mu \pm 1\sigma$
Same-sign dileptons	4.6	$1.7^{+0.9}_{-0.5}$	$2.7^{+1.1}_{-1.0}$
Trileptons	3.7	$2.3^{+1.2}_{-0.7}$	$1.3^{+1.2}_{-1.0}$
Combined categories	3.9	$1.4^{+0.7}_{-0.4}$	$2.3^{+0.9}_{-0.8}$
Combined with 2015 data	3.4	$1.3^{+0.6}_{-0.4}$	$2.0^{+0.8}_{-0.7}$

[CMS, 13 TeV, 12.9 fb^{-1}]

Significance wrt no-signal hypothesis: 3.2σ (CMS) , 2.8σ (ATLAS)

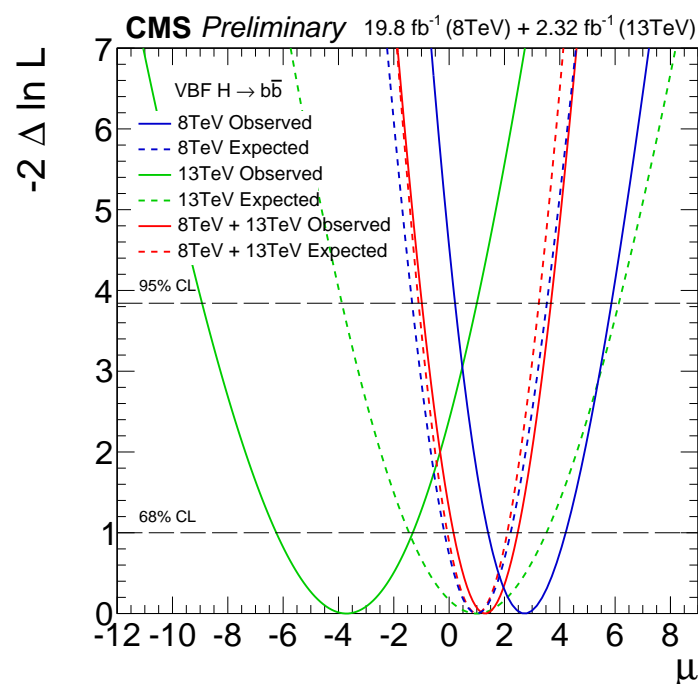
Search for $H \rightarrow b\bar{b}$

[CMS-PAS-HIG-16-003] , [JHEP01(2015)069 , ATLAS-CONF-2016-091]

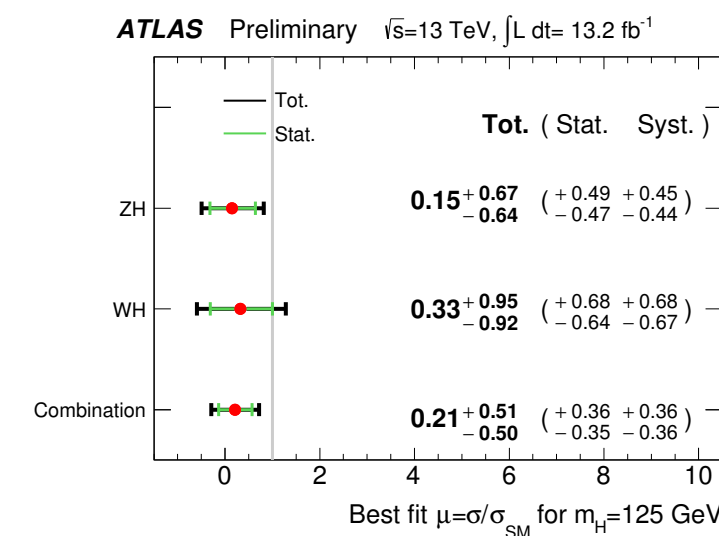
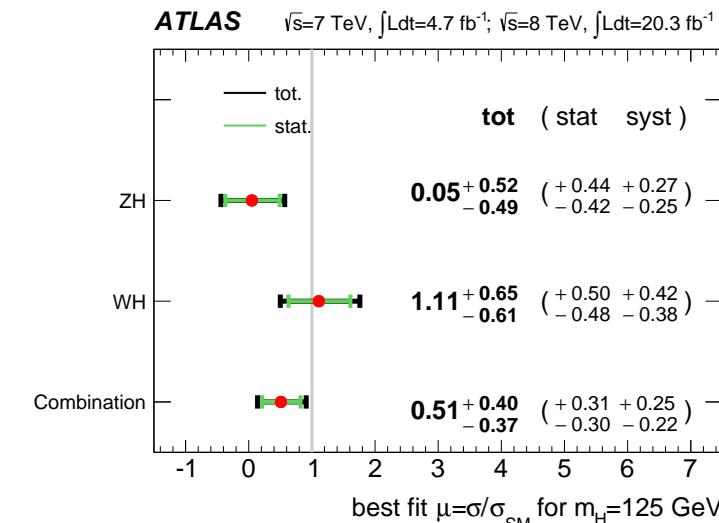
CMS: 8 TeV

H \rightarrow bb Channel	Best fit (68% CL)	Upper limits (95% CL)		Signal significance	
	Observed	Observed	Expected	Observed	Expected
VH	0.89 ± 0.43	1.68	0.85	2.08	2.52
tH	0.7 ± 1.8	4.1	3.5	0.37	0.58
VBF	$2.8^{+1.6}_{-1.4}$	5.5	2.5	2.20	0.83
Combined	$1.03^{+0.44}_{-0.42}$	1.77	0.78	2.56	2.70

CMS: 13 TeV (VBF production)



ATLAS: (VH production)

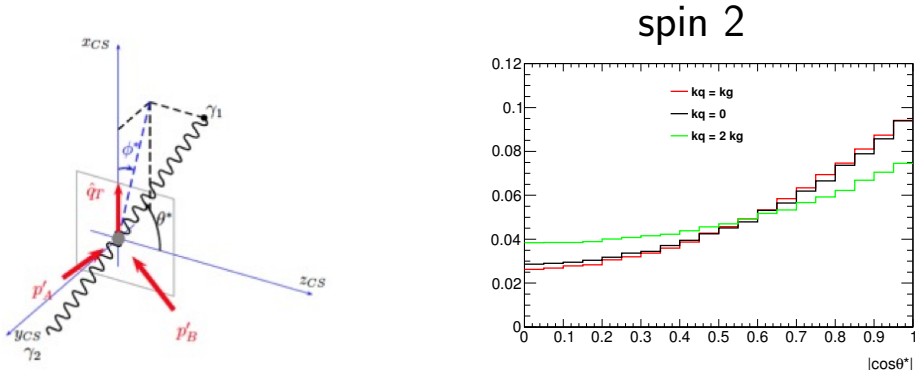


Spin hypothesis test and parity measurements

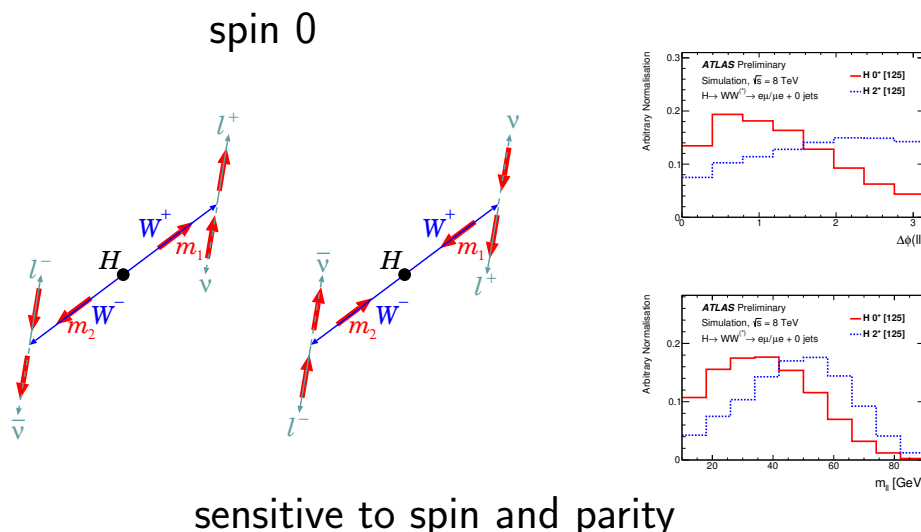
ATLAS: [Eur. Phys. J. C75 (2015) 476] , CMS: [PRD 92 (2015) 012004]

Spin/parity measurement

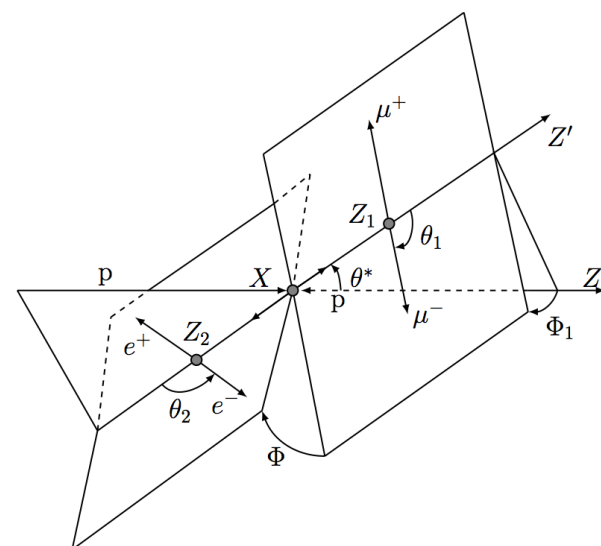
$H \rightarrow \gamma\gamma$: flat $|\cos\theta^*|$ for spin-0, sensitive to spin-2



$H \rightarrow WW^* \rightarrow \ell\nu\ell\nu$: W^+/W^- spin correlation



$H \rightarrow ZZ^* \rightarrow 4\ell$:



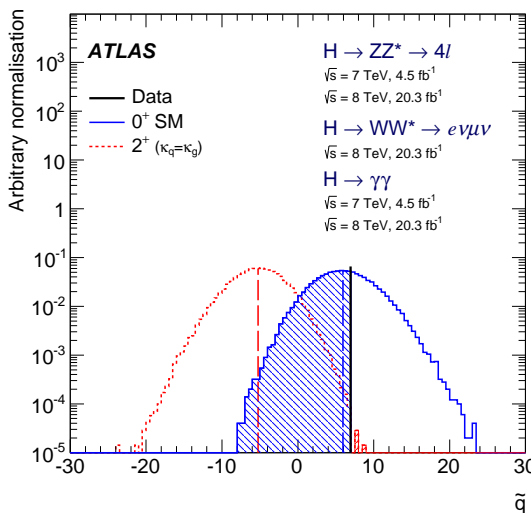
5 angular observables + m_{12} , m_{34}
can probe polarization of both H and Zs
sensitive to spin and parity

Spin-2 tests

effective lagrangian [HiggsCharacterization]

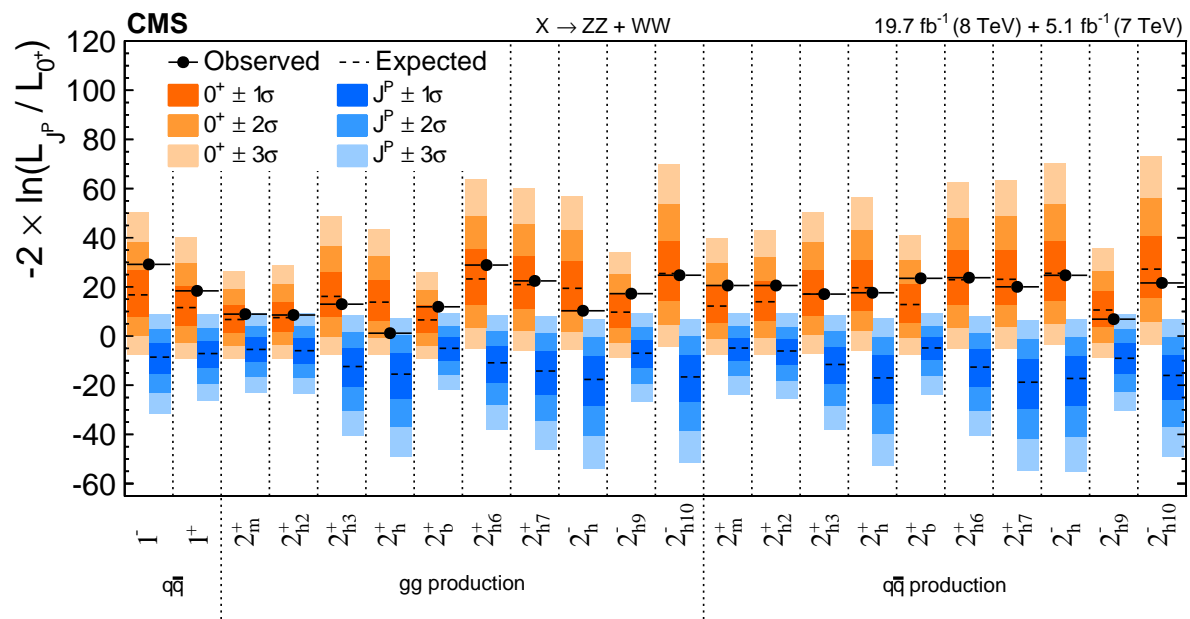
$$\mathcal{L}_2 = \frac{1}{\Lambda} \left[\sum_V \kappa_V X^{\mu\nu} \mathcal{T}_{\mu\nu}^V + \sum_f \kappa_f X^{\mu\nu} \mathcal{T}_{\mu\nu}^f \right]$$

[below, $\tilde{q} \equiv -2 \ln \left(\frac{L_{JP}}{L_{0^+}} \right)$]



effective transition amplitude [JHU]

$$\begin{aligned}
A(X_{J=2}VV) \sim & \Lambda^{-1} \left[2c_1^{VV} t_{\mu\nu} f^{*,1,\mu\alpha} f^{*,2,\nu\alpha} + 2c_2^{VV} t_{\mu\nu} \frac{q_\alpha q_\beta}{\Lambda^2} f^{*,1,\mu\alpha} f^{*,2,\nu\beta} \right. \\
& + c_3^{VV} t_{\beta\nu} \frac{\tilde{q}^\beta \tilde{q}^\alpha}{\Lambda^2} (f^{*,1,\mu\nu} f^{*,2}_{\mu\alpha} + f^{*,2,\mu\nu} f^{*,1}_{\mu\alpha}) + c_4^{VV} t_{\mu\nu} \frac{\tilde{q}^\nu \tilde{q}^\mu}{\Lambda^2} f^{*,1,\alpha\beta} f^{*,2}_{\alpha\beta} \\
& + m_V^2 \left(2c_5^{VV} t_{\mu\nu} \epsilon_{V1}^{*\mu} \epsilon_{V2}^{*\nu} + 2c_6^{VV} t_{\mu\nu} \frac{\tilde{q}^\mu q_\alpha}{\Lambda^2} (\epsilon_{V1}^{*\nu} \epsilon_{V2}^{*\alpha} - \epsilon_{V1}^{*\alpha} \epsilon_{V2}^{*\nu}) + c_7^{VV} t_{\mu\nu} \frac{\tilde{q}^\mu \tilde{q}^\nu}{\Lambda^2} \epsilon_{V1}^* \epsilon_{V2}^* \right) \\
& \quad \left. + c_8^{VV} t_{\mu\nu} \frac{\tilde{q}^\mu \tilde{q}^\nu}{\Lambda^2} f^{*,1,\alpha\beta} \tilde{f}_{\alpha\beta}^{*,2} \right. \\
& \quad \left. + m_V^2 \left(c_9^{VV} t^{\mu\alpha} \frac{\tilde{q}_\alpha \epsilon_{\mu\nu\rho\sigma} \epsilon_{V1}^{*\nu} \epsilon_{V2}^{*\rho} q^\sigma}{\Lambda^2} + c_{10}^{VV} t^{\mu\alpha} \frac{\tilde{q}_\alpha \epsilon_{\mu\nu\rho\sigma} q^\rho \tilde{q}^\sigma}{\Lambda^4} (\epsilon_{V1}^{*\nu} (q \epsilon_{V2}^*) + \epsilon_{V2}^{*\nu} (q \epsilon_{V1}^*)) \right) \right]
\end{aligned}$$



⇒ **data favour spin-0**

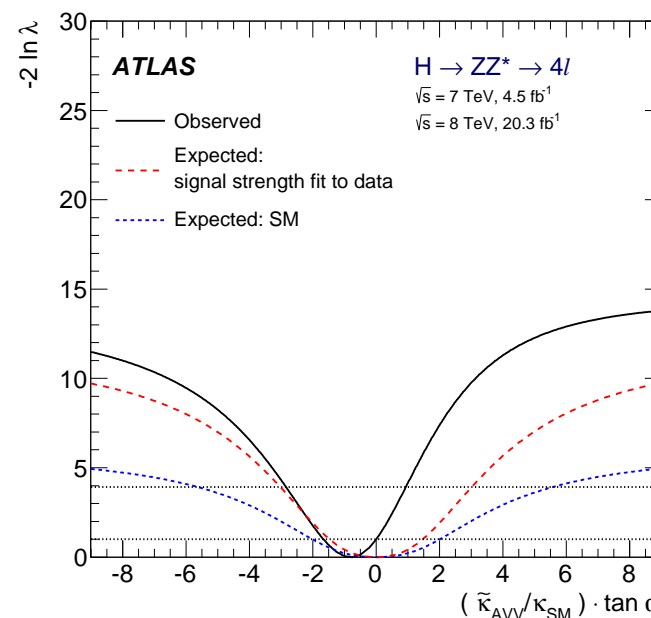
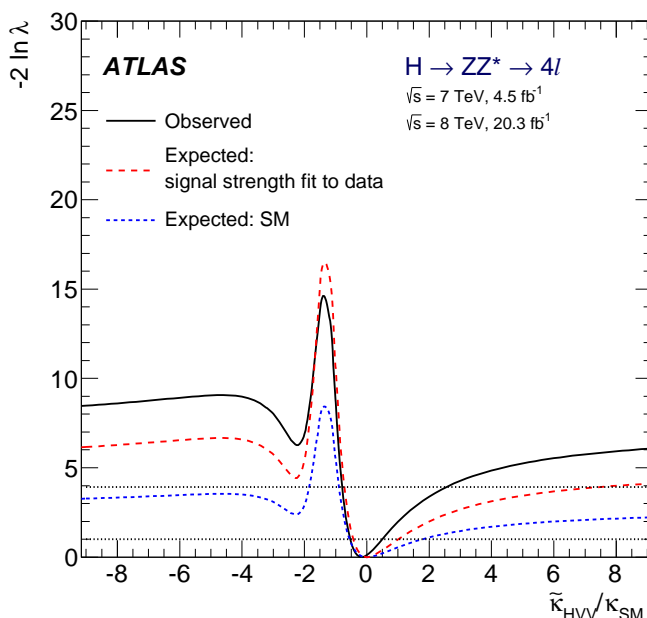
Parity and CP-mixing

$$\mathcal{L}_0^V = \chi_0 \cdot \left\{ \cos \alpha \kappa_{SM} \left[\frac{1}{2} g_{HZZ} Z_\mu Z^\mu + g_{HWV} W_\mu^+ W^{-\mu} \right] \right. \\ \left. - \frac{1}{4\Lambda} \left[\cos \alpha \kappa_{HZZ} Z_{\mu\nu} Z^{\mu\nu} + \sin \alpha \kappa_{AZZ} Z_{\mu\nu} \tilde{Z}^{\mu\nu} \right] \right. \\ \left. - \frac{1}{2\Lambda} \left[\cos \alpha \kappa_{HWV} W_{\mu\nu}^+ W^{-\mu\nu} + \sin \alpha \kappa_{AWV} W_{\mu\nu}^+ \tilde{W}^{-\mu\nu} \right] \right\}$$

Standard Model : $\alpha = 0$, $\kappa_{HVV} = 0$, $\kappa_{AVV} = 0$

Beyond SM : $\kappa_{HVV} \Rightarrow CP\text{-even}$, $\kappa_{AVV} \Rightarrow CP\text{-odd}$

CP-mixing for $\alpha \neq 0$ and $\alpha \neq \frac{\pi}{2}$



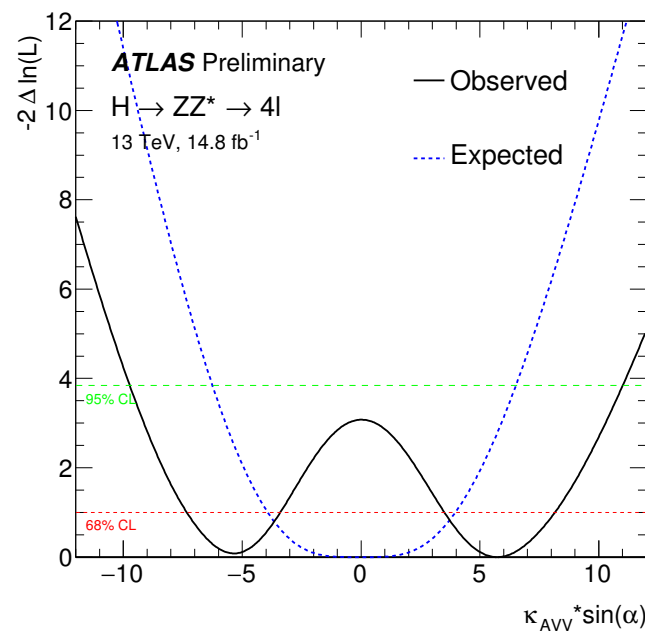
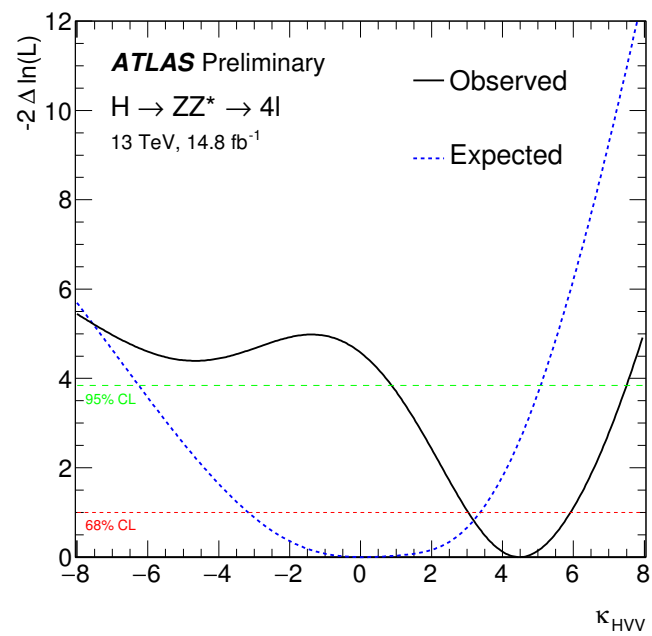
$$\tilde{\kappa}_{HVV} = \frac{v}{4\Lambda} \kappa_{HVV}$$

$$\tilde{\kappa}_{AVV} = \frac{v}{4\Lambda} \kappa_{AVV}$$

$\Rightarrow \tilde{\kappa}_{HVV}, \tilde{\kappa}_{AVV}$ compatible with 0

CP-tests at 13 TeV

[ATLAS-CONF-2016-079]



Some “tension” for $\kappa_{HVV}, \sim 2.1\sigma$
... not worrisome at this stage, though

Width measurement

Width measurement

[Phys. Lett. B 736 (2014) 64]

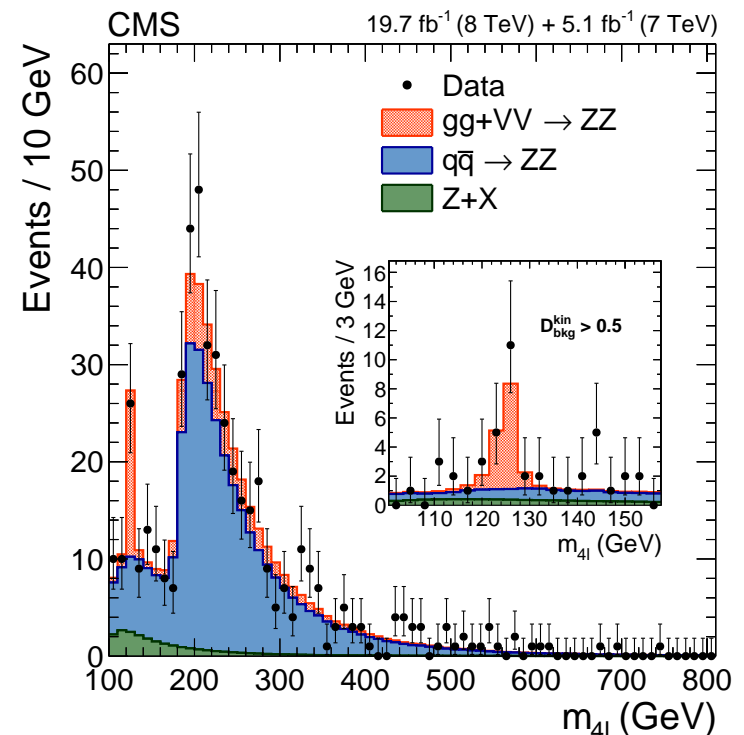
In Standard Model, the Higgs decay width is expected to be $\Gamma_H \simeq 4$ MeV

\Rightarrow cannot measure it from the observed resonance width (experimental uncertainty $\mathcal{O}(\text{GeV})$)

Use $H \rightarrow ZZ^{(*)} \rightarrow 4\ell$ decays.

Compare Higgs on-shell ($gg \rightarrow H \rightarrow ZZ^*$) and off-shell ($gg \rightarrow H^* \rightarrow ZZ$) production cross-sections:

$$\sigma_{gg \rightarrow H \rightarrow ZZ^*} \propto \frac{g_{Hgg} \cdot g_{HZZ}}{\Gamma_H m_H} \quad ; \quad \sigma_{gg \rightarrow H^* \rightarrow ZZ} \propto \frac{g_{Hgg} \cdot g_{HZZ}}{(2m_Z)^2}$$

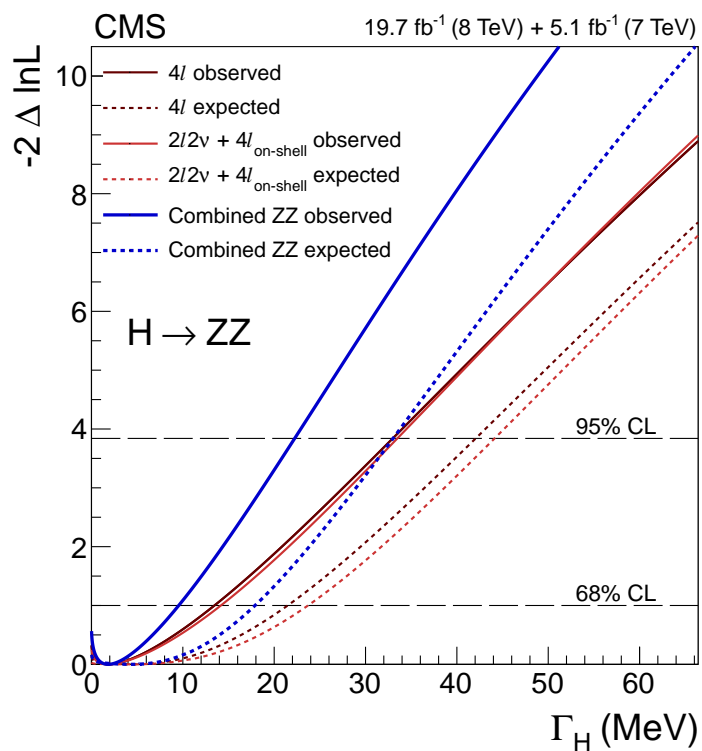


\Rightarrow under specific assumptions on how g_{Hgg} , g_{HZZ} scale with \hat{s} , $\frac{\sigma_{gg \rightarrow H^* \rightarrow ZZ}}{\sigma_{gg \rightarrow H \rightarrow ZZ^*}}$ gives a measurement of Γ_H

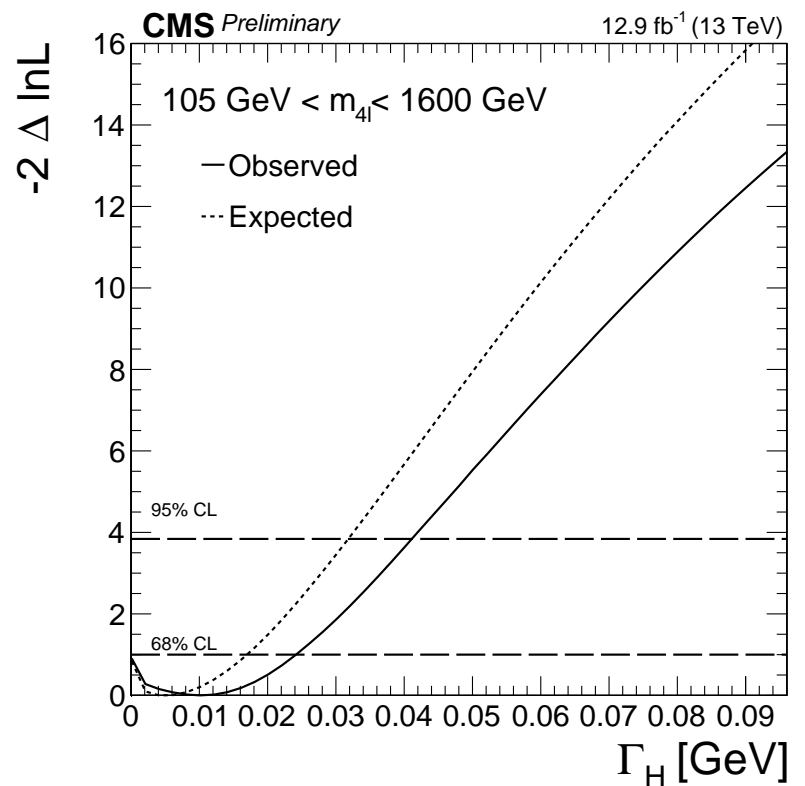
Total width at 8 and 13 TeV

[Phys. Lett. B 736 (2014) 64 , CMS-PAS-HIG-16-033]

8 TeV



13 TeV



⇒ $\Gamma_H < 22$ MeV (at 95% CL)

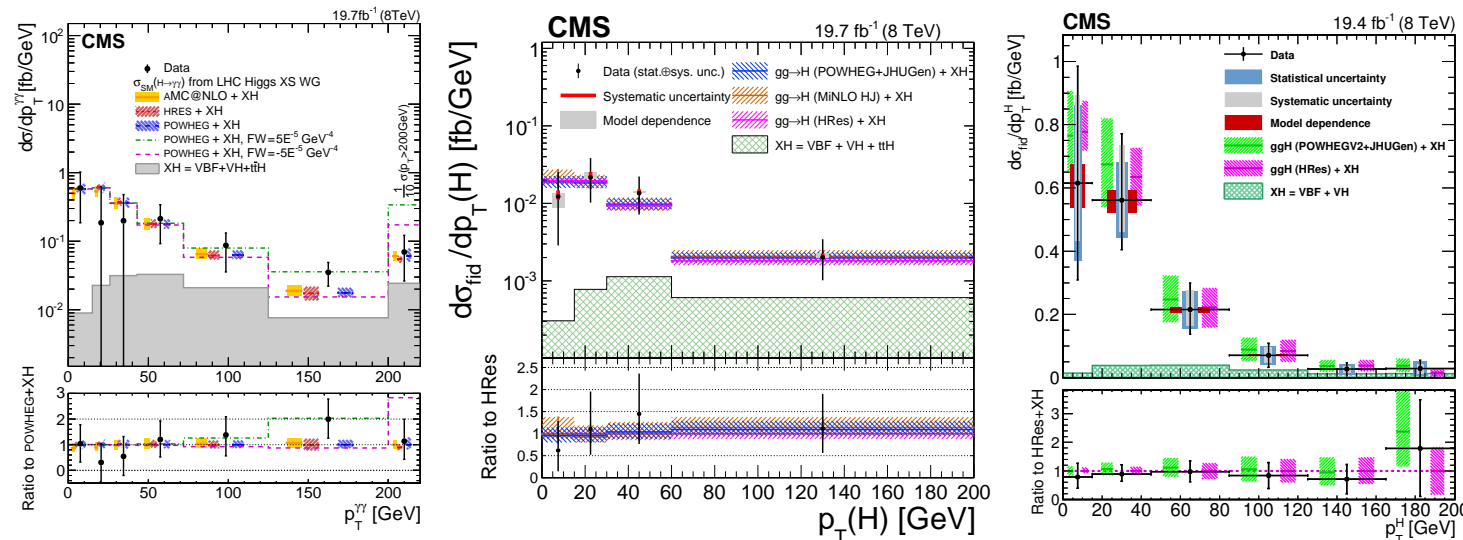
⇒ $\Gamma_H < 41$ MeV (at 95% CL)

Differential cross-sections

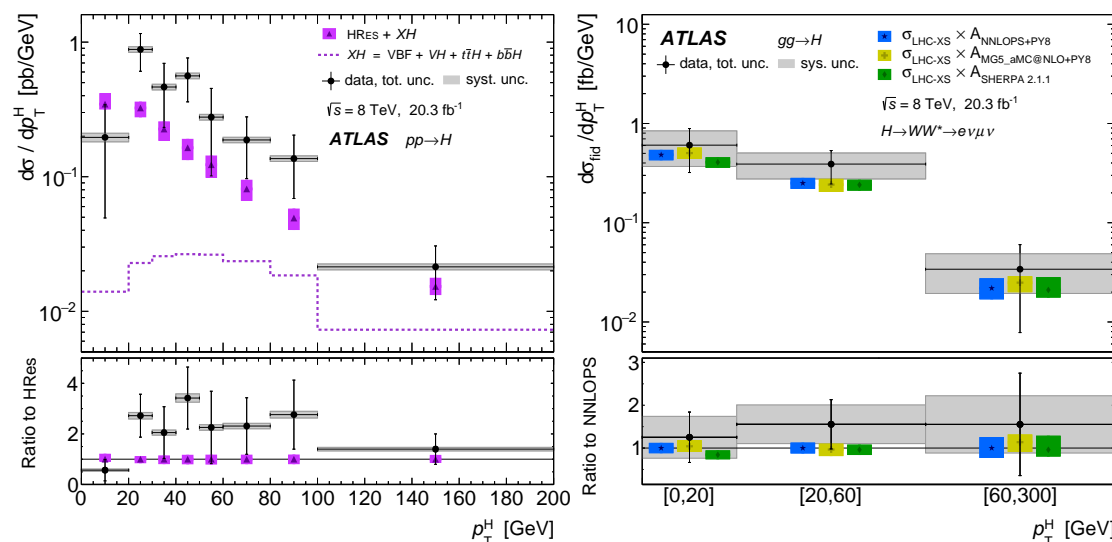
Differential cross-sections @ Run-I

[EPJC 76 (2016) 13 , JHEP 04 (2016) 005 , HIG-15-010] , [Phys. Rev. Lett. 115 (2015) 091801 , arXiv:1604.02997]

CMS: $H \rightarrow \gamma\gamma$, $H \rightarrow 4\ell$, $H \rightarrow WW^* \rightarrow e\nu\mu\nu$

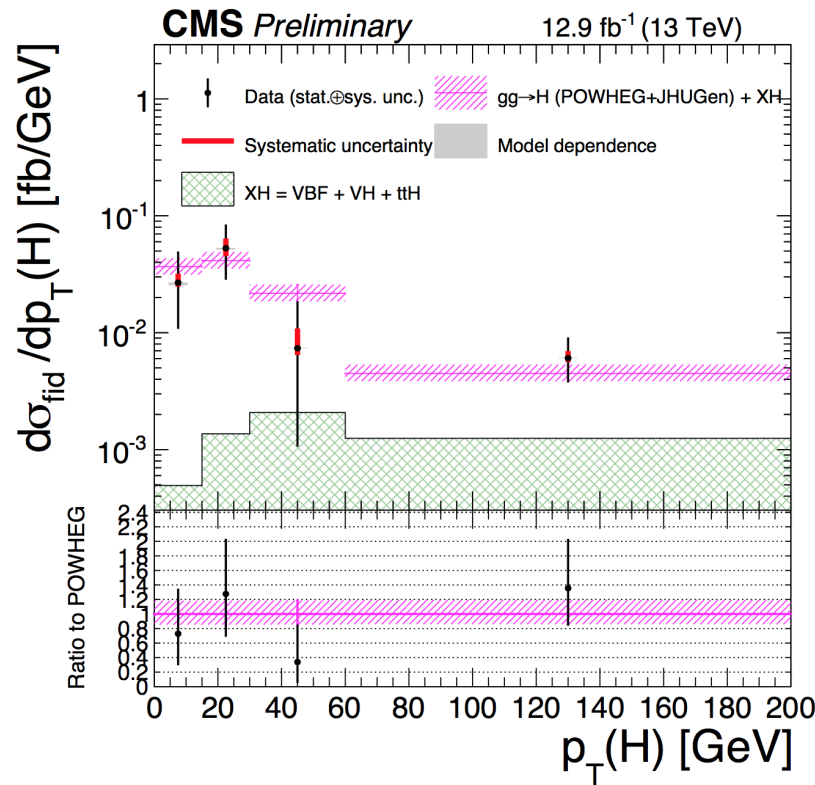


ATLAS: $H \rightarrow \gamma\gamma$, $H \rightarrow 4\ell$ combined, $H \rightarrow WW^* \rightarrow e\nu\mu\nu$

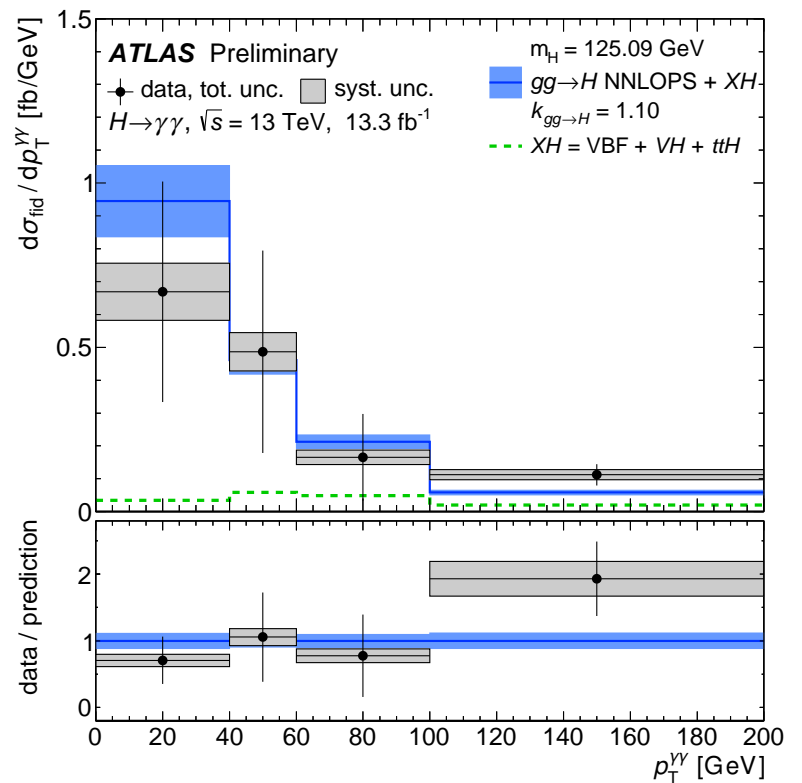


Differential cross-sections at 13 TeV

$H \rightarrow ZZ^* \rightarrow 4\ell$



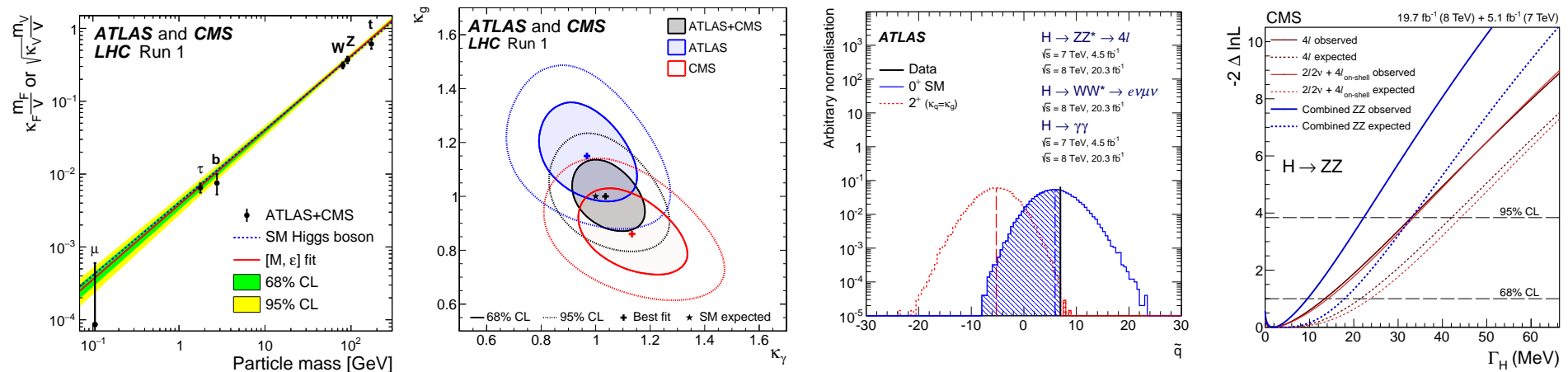
$H \rightarrow \gamma\gamma$



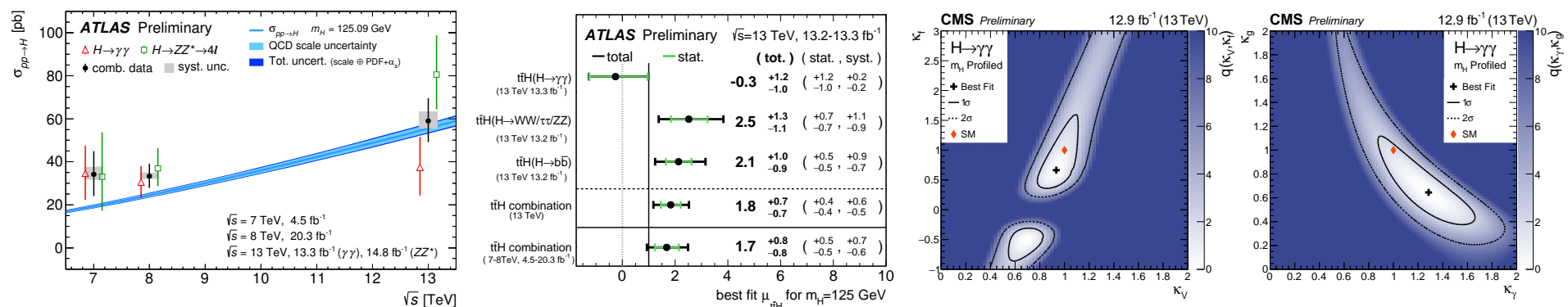
Conclusions

Conclusions

Run-I analyses well mature, ATLAS+CMS combined results available for mass and couplings:



Run-II: efficient data-taking, analyses progressing fast, (cross-section) \times (luminosity) already beat Run-I



⇒ We are still compatible with Standard Model prediction . . . but uncertainties are still large.

Theory uncertainties improved a lot. Important to pursue precision measurements in the Higgs sector, in Run-II and beyond, to investigate possible deviations from SM

Thanks for your attention

More material

Statistical models used in measurements

Extended likelihood function: $\mathcal{L}(\vec{\alpha}; \vec{\nu})$:

$$-\ln \mathcal{L}(\vec{\alpha}; \vec{\nu}) = (n_s + n_b) - \sum_e \left[\overbrace{n_s \cdot f_s(\vec{x}_e | \vec{\alpha}, \vec{\nu}_s)}^{\text{signal pdf}} + \overbrace{n_b \cdot f_b(\vec{x}_e | \vec{\nu}_b)}^{\text{background pdf}} \right] - \underbrace{\sum_k \ln \pi_k(\nu_k)}_{\text{ancillary pdfs}}$$

- n_s, n_b : signal / background yields
- \vec{x} : observables
- f_s, f_b : signal / background pdfs
- $\vec{\alpha}$: parameters of interest
(mass, cross-section, couplings, . . .)
- $\vec{\nu}$: “nuisance parameters”
(shape parameters, systematics, . . .)
- π_k : pdfs obtained from auxiliary measurements

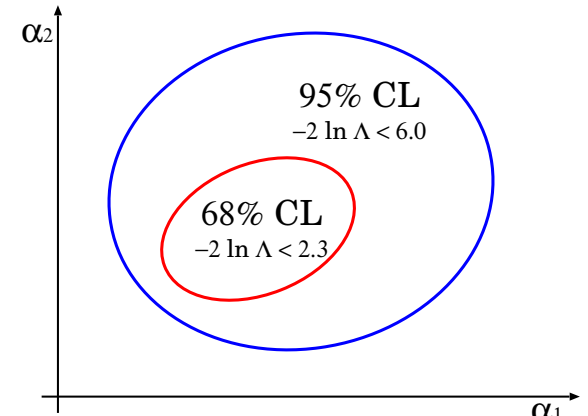
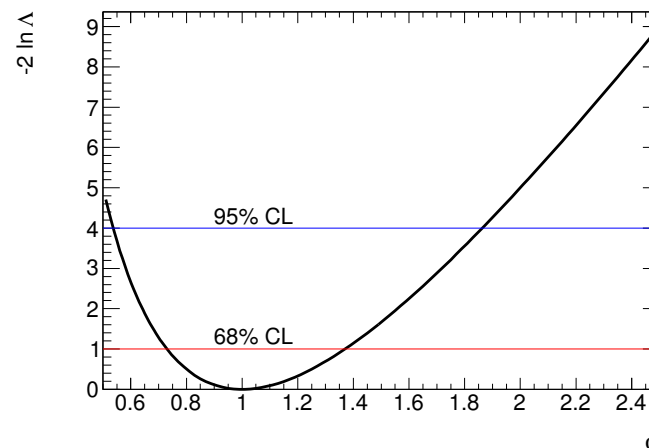
Test statistic: “Profiled Likelihood Ratio” (PLR)

$$q_{\vec{\alpha}} = -2 \ln \Lambda(\vec{\alpha}) = -2 \ln \frac{\mathcal{L}(\vec{\alpha}; \hat{\vec{\nu}}(\vec{\alpha}))}{\mathcal{L}(\hat{\vec{\alpha}}; \hat{\vec{\nu}})}$$

- $\leftarrow \mathcal{L}(\vec{\alpha}; \hat{\vec{\nu}}(\vec{\alpha}))$: likelihood for fixed $\vec{\alpha}$ and “profiled” $\vec{\nu}$
- $\leftarrow \mathcal{L}(\hat{\vec{\alpha}}; \hat{\vec{\nu}})$: maximum likelihood for free $\vec{\alpha}, \vec{\nu}$

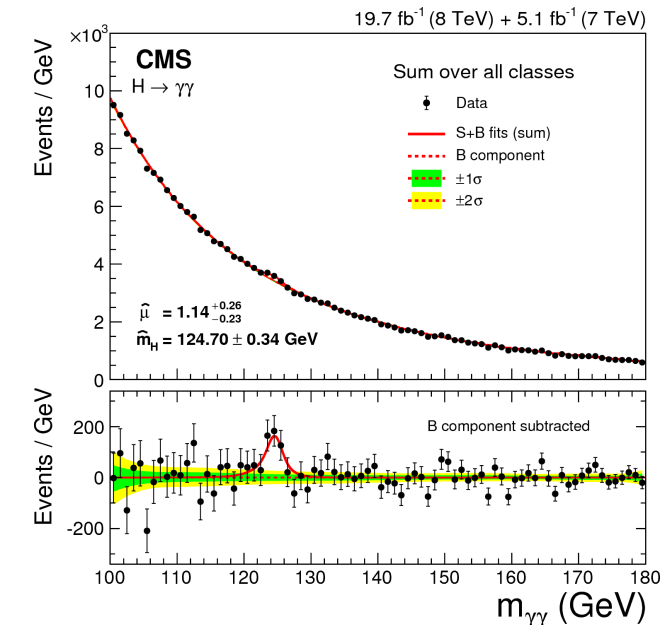
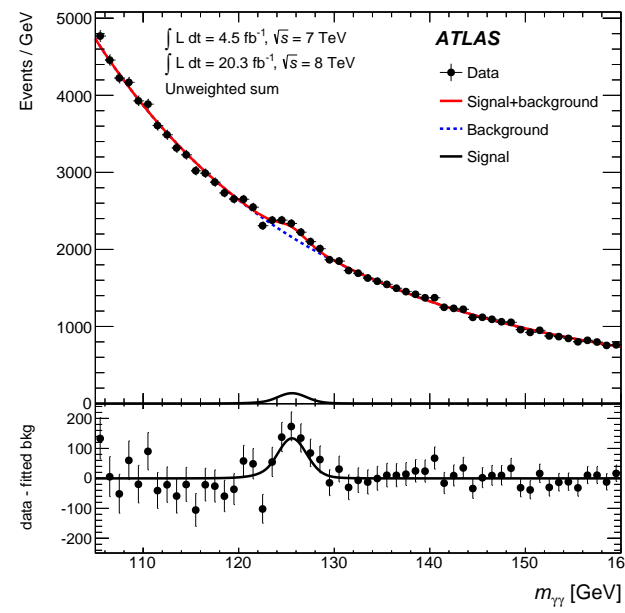
Wilks' theorem : if $\vec{\alpha} = \vec{\alpha}^{true}$, then $q_{\vec{\alpha}}$ follows a χ_D^2 distribution, with D being the number of parameters of interest $\vec{\alpha}$

⇒ compute confidence intervals for $\vec{\alpha}$

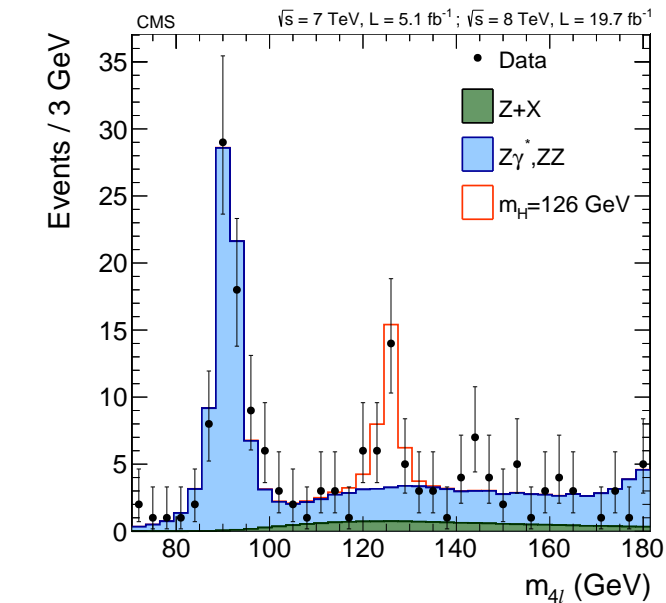
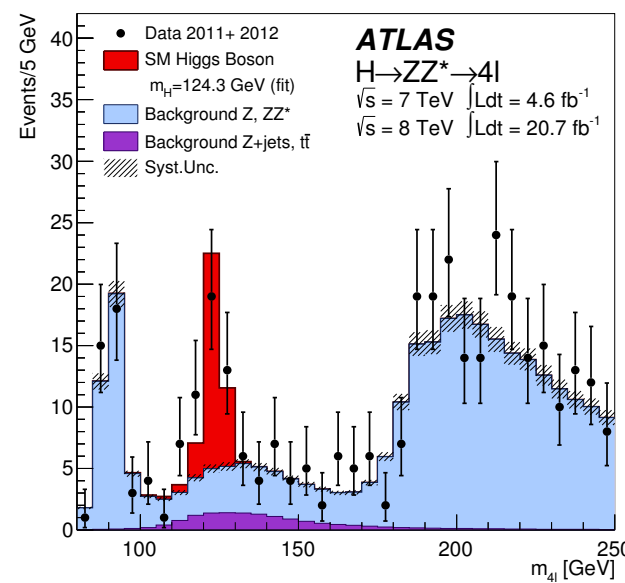


Higgs observation in Run-I : $H \rightarrow \gamma\gamma$ and $H \rightarrow ZZ^* \rightarrow 4\ell$

$H \rightarrow \gamma\gamma$

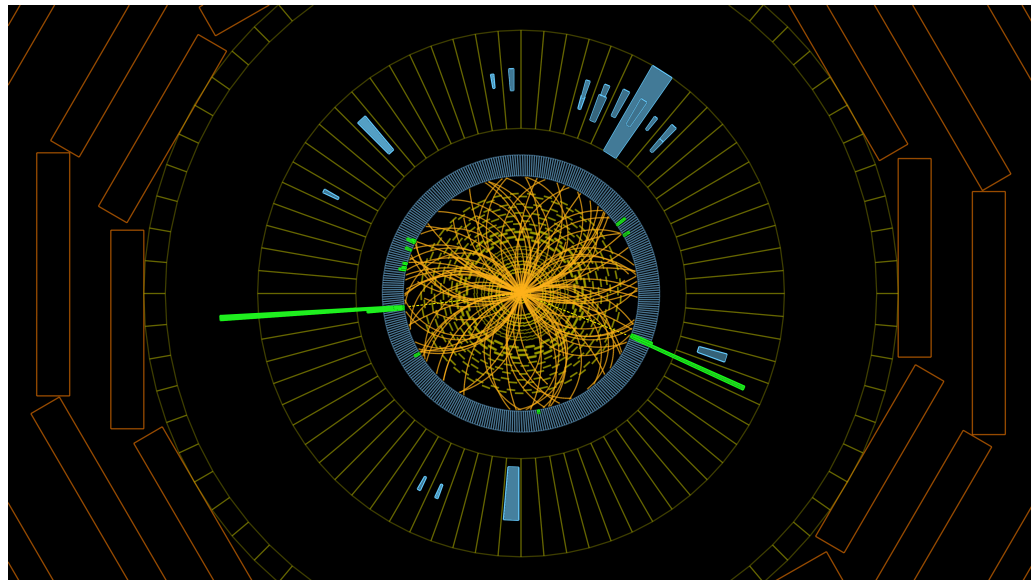


$H \rightarrow 4\ell$

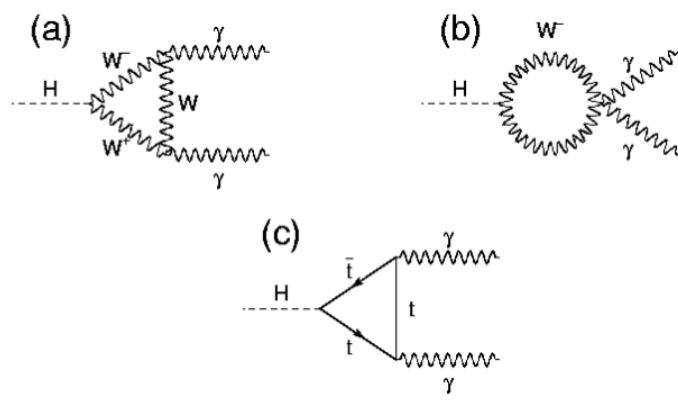
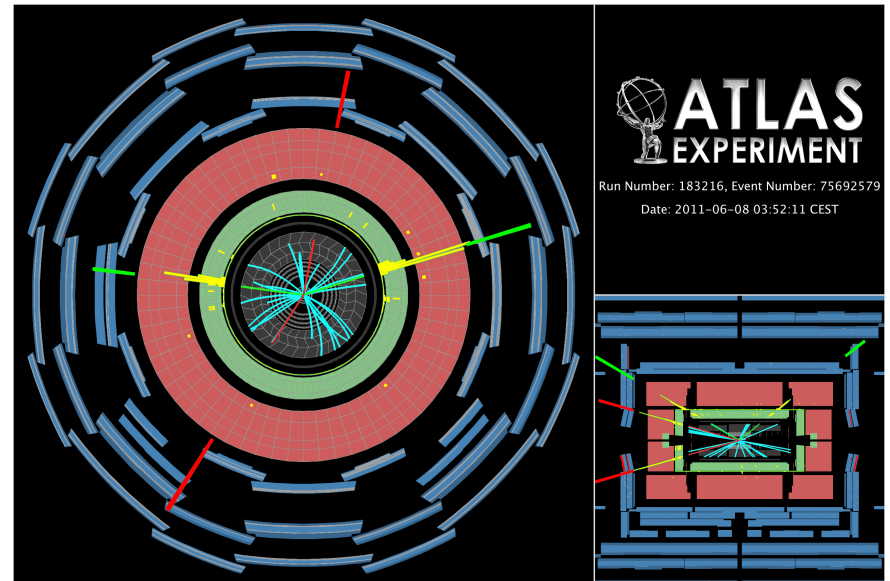


Higgs candidates : $H \rightarrow \gamma\gamma$ and $H \rightarrow ZZ^* \rightarrow 4\ell$

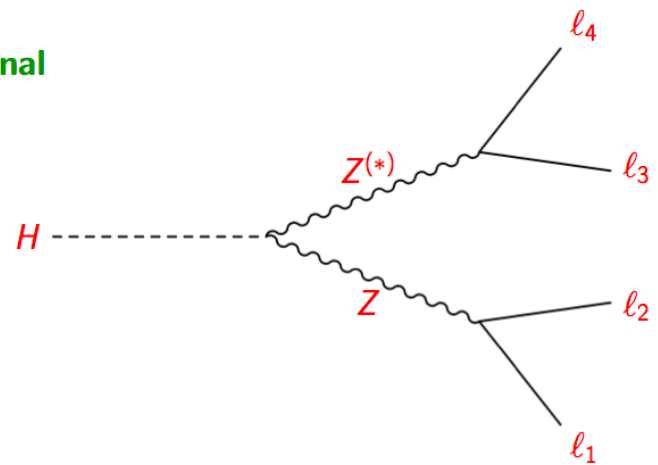
$H \rightarrow \gamma\gamma$ candidate at CMS



$H \rightarrow ZZ^* \rightarrow e^+e^-\mu^+\mu^-$ candidate at ATLAS



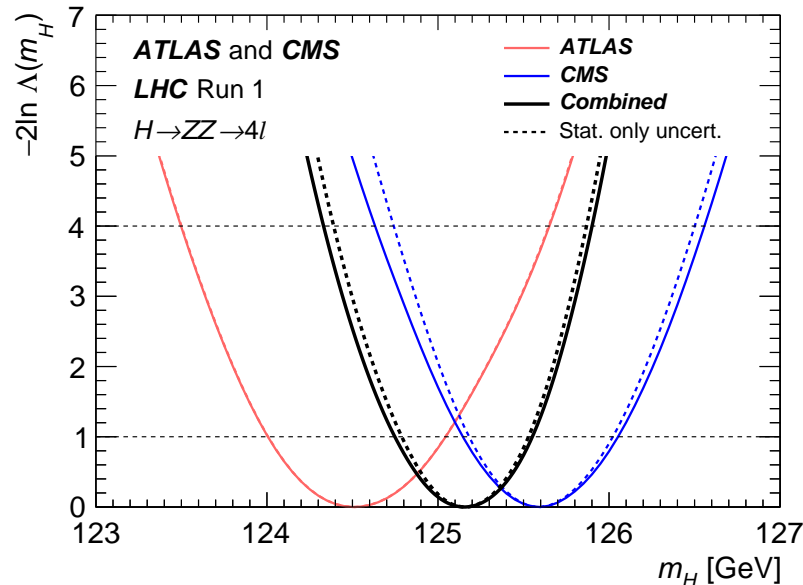
Signal



Mass measurement

Use the $H \rightarrow \gamma\gamma$ and $H \rightarrow ZZ^* \rightarrow 4\ell$ decay channels
that allow a full kinematics reconstruction with good invariant mass resolution ($\mathcal{O}(1 \text{ GeV})$)

4 ℓ channel

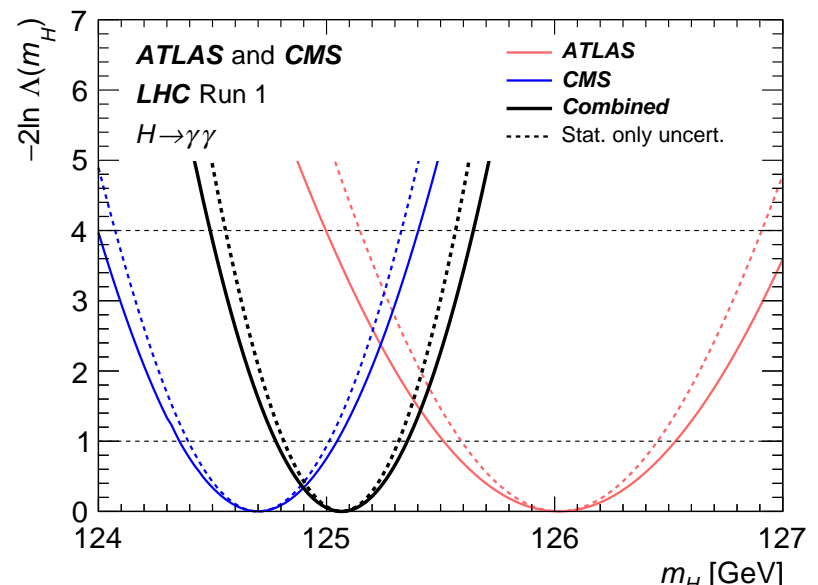


$$\hat{m}_H^{4\ell} = 125.15 \pm 0.37(\text{stat}) \pm 0.15(\text{syst}) \text{ GeV}$$

Good signal/background, low statistics

e, μ energy scales from $J/\psi, \Upsilon, Z \rightarrow \ell\ell$

$\gamma\gamma$ channel



$$\hat{m}_H^{\gamma\gamma} = 125.07 \pm 0.25(\text{stat}) \pm 0.14(\text{syst}) \text{ GeV}$$

Large background, good statistics

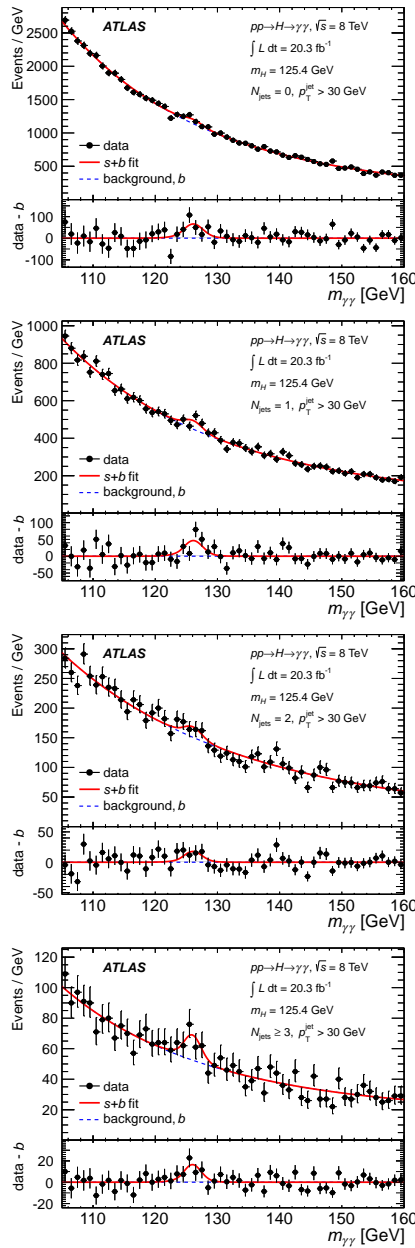
γ energy scale from $Z \rightarrow e^+e^-$ and $e \rightarrow \gamma$ extrapolation

Comparison with SM expectations

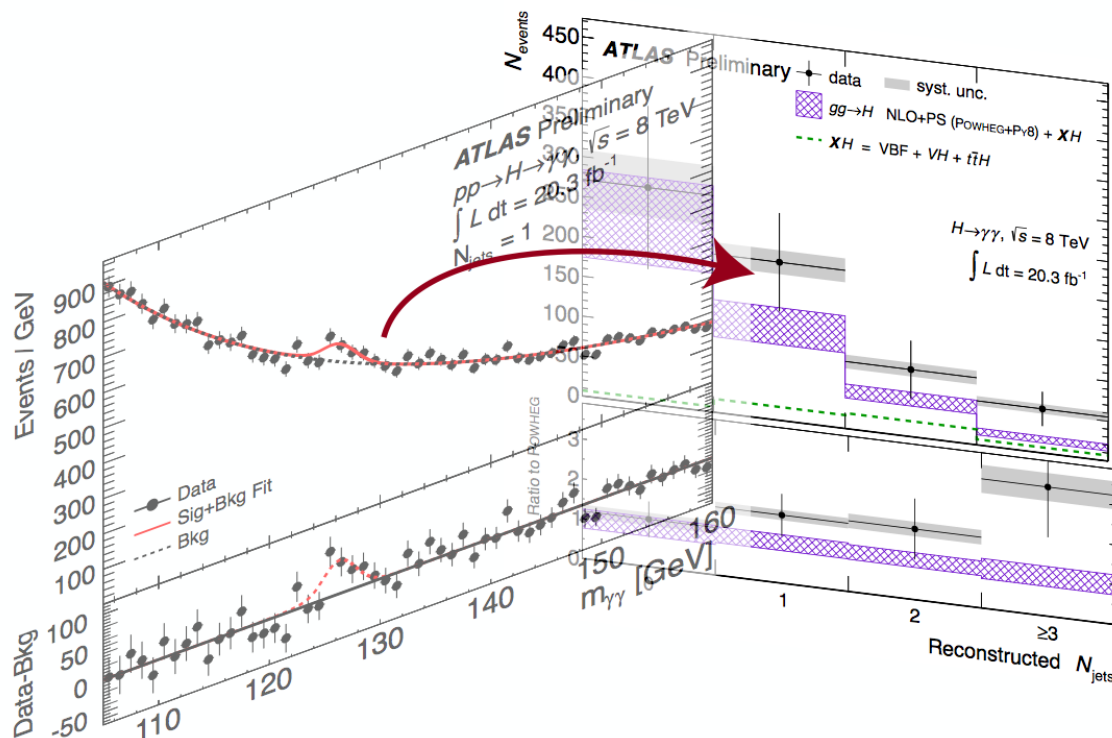
Parameterisation	<i>p</i> -value	DOF	Parameters
Global signal strength	40%	1	μ
Production processes	24%	5	$\mu_{ggF}, \mu_{VBF}, \mu_{WH}, \mu_{ZH}, \mu_{ttH}$
Decay modes	65%	5	$\mu^{\gamma\gamma}, \mu^{ZZ}, \mu^{WW}, \mu^{\tau\tau}, \mu^{bb}$
Decay modes with $H \rightarrow \mu\mu$	75%	6	$\mu^{\gamma\gamma}, \mu^{ZZ}, \mu^{WW}, \mu^{\tau\tau}, \mu^{bb}, \mu^{\mu\mu}$
μ_V and μ_F per decay	90%	10	$\mu_V^{\gamma\gamma}, \mu_V^{ZZ}, \mu_V^{WW}, \mu_V^{\tau\tau}, \mu_V^{bb}, \mu_F^{\gamma\gamma}, \mu_F^{ZZ}, \mu_F^{WW}, \mu_F^{\tau\tau}, \mu_F^{bb}$
μ_V/μ_F ratio	75%	6	$\mu_V/\mu_F, \mu_F^{\gamma\gamma}, \mu_F^{ZZ}, \mu_F^{WW}, \mu_F^{\tau\tau}, \mu_F^{bb}$
$\sigma_i \cdot B^f$ product	20%	23	$(\sigma \cdot B)^{\gamma\gamma}_{ggF}, (\sigma \cdot B)^{ZZ}_{ggF}, (\sigma \cdot B)^{WW}_{ggF}, (\sigma \cdot B)^{\tau\tau}_{ggF}, (\sigma \cdot B)^{\gamma\gamma}_{VBF},$ $(\sigma \cdot B)^{ZZ}_{VBF}, (\sigma \cdot B)^{WW}_{VBF}, (\sigma \cdot B)^{\tau\tau}_{VBF}, (\sigma \cdot B)^{\gamma\gamma}_{WH},$ $(\sigma \cdot B)^{ZZ}_{WH}, (\sigma \cdot B)^{WW}_{WH}, (\sigma \cdot B)^{\tau\tau}_{WH}, (\sigma \cdot B)^{bb}_{WH},$ $(\sigma \cdot B)^{\gamma\gamma}_{ZH}, (\sigma \cdot B)^{ZZ}_{ZH}, (\sigma \cdot B)^{WW}_{ZH}, (\sigma \cdot B)^{\tau\tau}_{ZH}, (\sigma \cdot B)^{bb}_{ZH},$ $(\sigma \cdot B)^{\gamma\gamma}_{ttH}, (\sigma \cdot B)^{ZZ}_{ttH}, (\sigma \cdot B)^{WW}_{ttH}, (\sigma \cdot B)^{\tau\tau}_{ttH}, (\sigma \cdot B)^{bb}_{ttH}$
Ratios of σ and BR relative to $\sigma(gg \rightarrow H \rightarrow ZZ)$	16%	9	$\sigma(gg \rightarrow H \rightarrow ZZ), \sigma_{VBF}/\sigma_{ggF}, \sigma_{WH}/\sigma_{ggF}, \sigma_{ZH}/\sigma_{ggF},$ $\sigma_{ttH}/\sigma_{ggF}, B^{WW}/B^{ZZ}, B^{\gamma\gamma}/B^{ZZ}, B^{\tau\tau}/B^{ZZ}, B^{bb}/B^{ZZ}$
Ratios of σ and BR relative to $\sigma(gg \rightarrow H \rightarrow ZZ)$ and 7/8 TeV	26%	14	$\sigma(gg \rightarrow H \rightarrow ZZ), \sigma_{VBF}/\sigma_{ggF}, \sigma_{WH}/\sigma_{ggF}, \sigma_{ZH}/\sigma_{ggF},$ $\sigma_{ttH}/\sigma_{ggF}, B^{WW}/B^{ZZ}, B^{\gamma\gamma}/B^{ZZ}, B^{\tau\tau}/B^{ZZ}, B^{bb}/B^{ZZ},$ $\sigma_{ggF}^{7\text{TeV}}/\sigma_{ggF}^{8\text{TeV}}, \sigma_{VBF}^{7\text{TeV}}/\sigma_{VBF}^{8\text{TeV}}, \sigma_{WH}^{7\text{TeV}}/\sigma_{WH}^{8\text{TeV}}, \sigma_{ZH}^{7\text{TeV}}/\sigma_{ZH}^{8\text{TeV}},$ $\sigma_{ttH}^{7\text{TeV}}/\sigma_{ttH}^{8\text{TeV}}$
Coupling ratios	12%	7	$\kappa_g z, \lambda_z g, \lambda_t g, \lambda_w z, \lambda_{\gamma z}, \lambda_{\tau z}, \lambda_b z$
Couplings, SM loops	74%	6	$\kappa_Z, \kappa_W, \kappa_t, \kappa_\tau, \kappa_b, \kappa_\mu$
Couplings vs mass	55%	2	M, ϵ
Couplings, BSM loops	11%	7	$\kappa_Z, \kappa_W, \kappa_t, \kappa_\tau, \kappa_b, \kappa_g, \kappa_\gamma$
BSM loops only	87%	2	κ_g, κ_γ
Fermion and vector couplings	64%	2	$\lambda_{FV}, \kappa_{VV}$
Up vs down couplings	72%	3	$\lambda_{du}, \lambda_{Vu}, \kappa_{uu}$
Lepton vs quark couplings	79%	3	$\lambda_{lq}, \lambda_{Vq}, \kappa_{qq}$

“Compatibility with the SM prediction of fit results as a whole under the asymptotic approximation. For each parameterisation, the unconditional best fit is compared with the conditional fit where all parameters are set to their SM values. The conversion from $-2 \ln \Lambda$ to the quoted *p*-values is performed assuming a two-sided distribution with the specified number of degrees of freedom (DOF). The quoted *p*-values are partially correlated between the different parameterisations.”

Extraction of signal yield per category ...



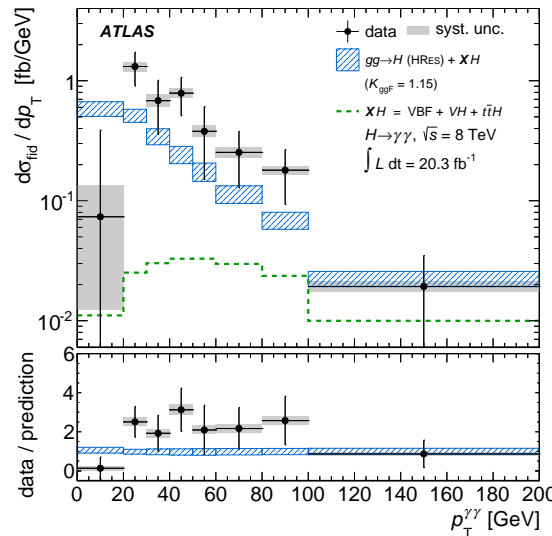
- divide events in categories (e.g. number of jets, bins of $p_T^{\gamma\gamma}$, bins of $Y_{\gamma\gamma}$, etc ...)
 - from the invariant mass spectrum, extract the signal yield in each category / bin



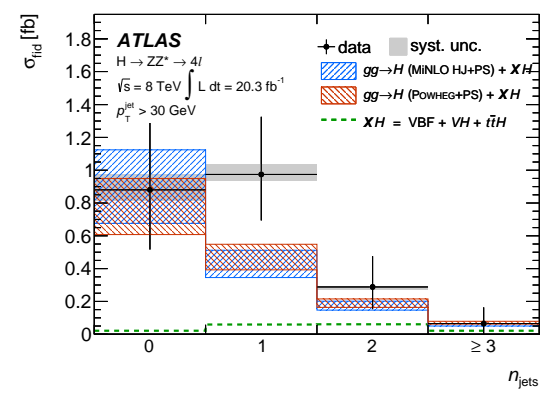
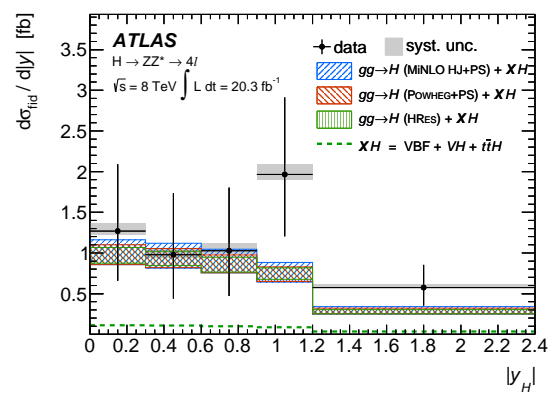
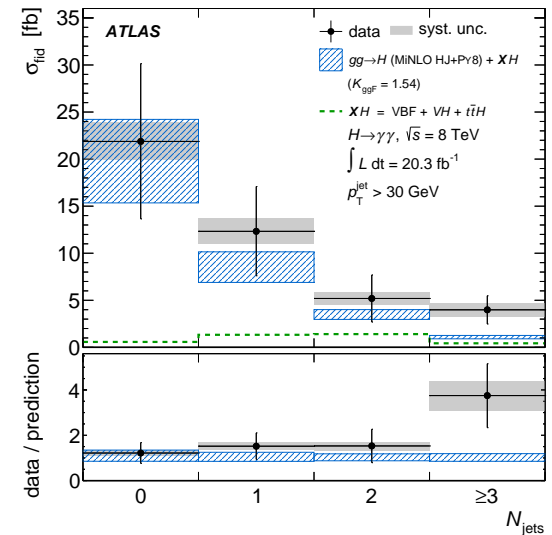
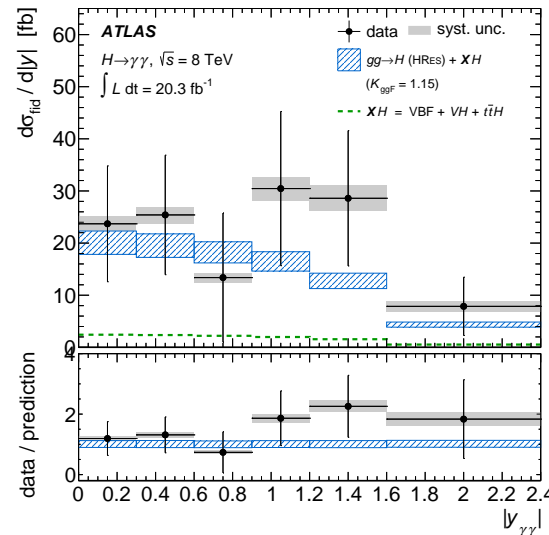
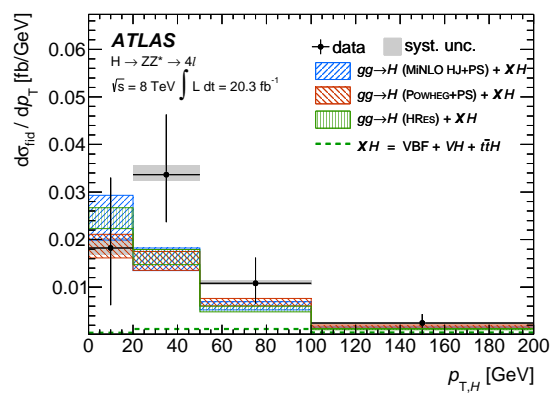
- then unfold the experimental effects (efficiencies, migrations, . . .)
 ⇒ get the cross-section per category / bin

Differential cross-sections

$$H \rightarrow \gamma\gamma$$

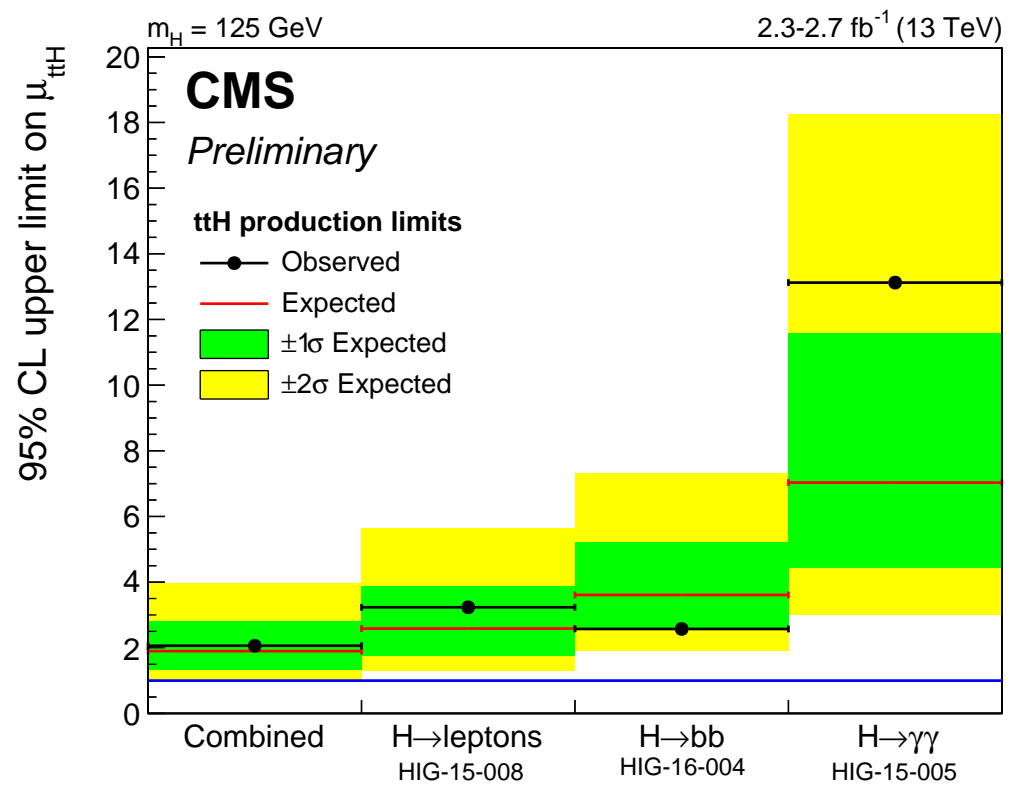
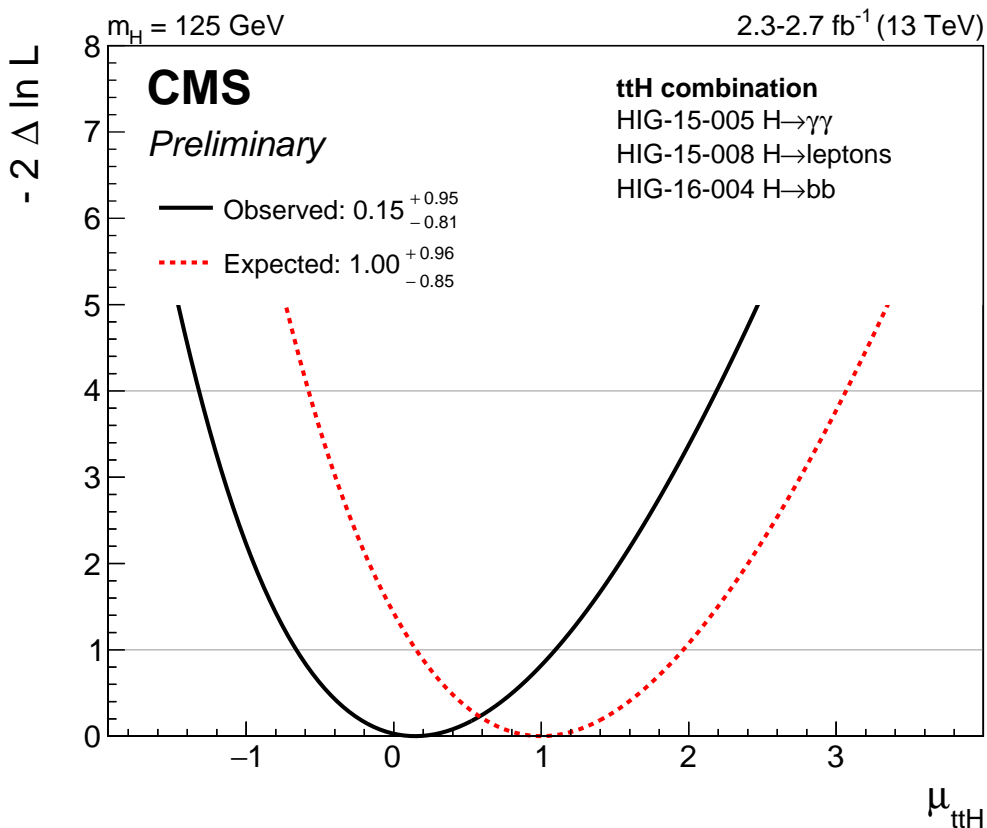


$H \rightarrow ZZ^* \rightarrow 4\ell$



ttH production

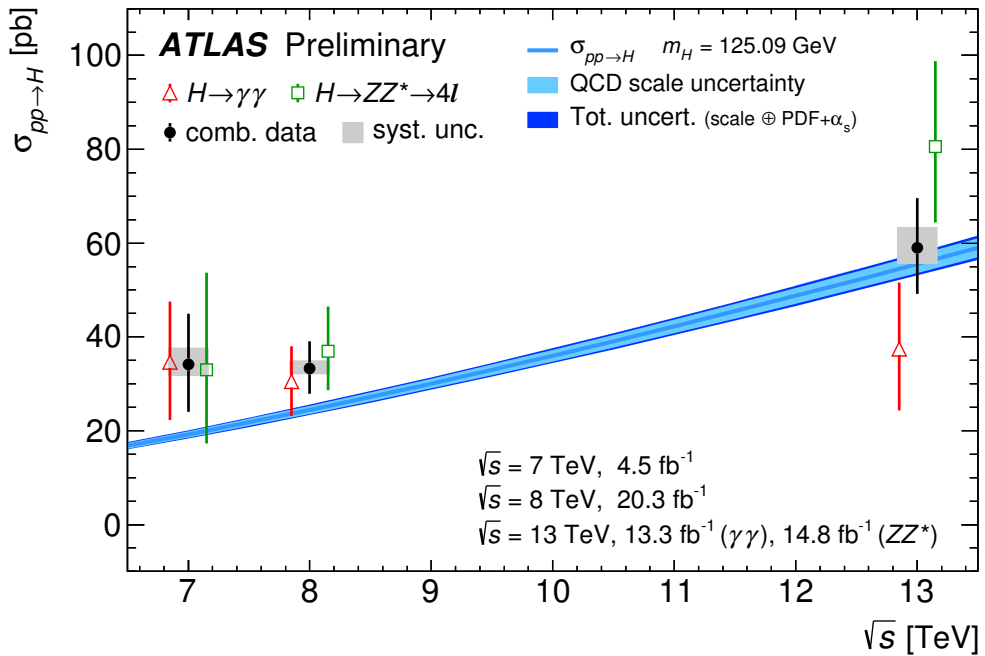
[HIG-15-008 , HIG-16-004 , HIG-15-005]



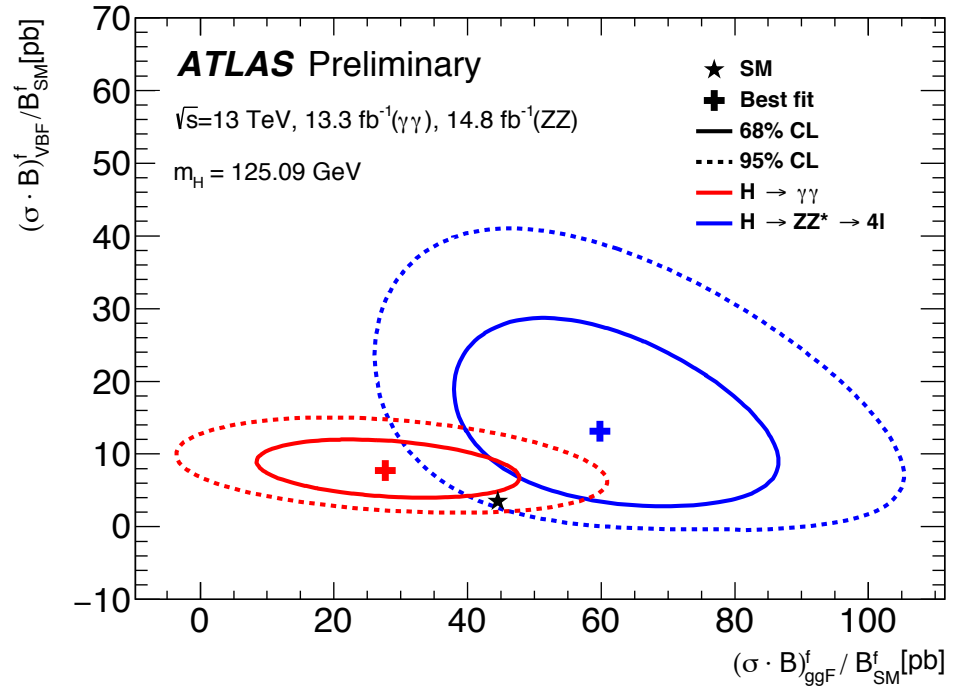
[to be updated if new results arrive from CMS 2016 data]

Total cross-section from $\gamma\gamma$ and 4ℓ final states

[ATLAS-CONF-2016-081]



Decay channel	Total cross section ($pp \rightarrow H + X$)		
	$\sqrt{s} = 7$ TeV	$\sqrt{s} = 8$ TeV	$\sqrt{s} = 13$ TeV
$H \rightarrow \gamma\gamma$	$35^{+13}_{-12} \text{ pb}$	$30.5^{+7.5}_{-7.4} \text{ pb}$	$37^{+14}_{-13} \text{ pb}$
$H \rightarrow ZZ^* \rightarrow 4\ell$	$33^{+21}_{-16} \text{ pb}$	37^{+9}_{-8} pb	$81^{+18}_{-16} \text{ pb}$
Combination	$34 \pm 10 \text{ (stat.)} {}^{+4}_{-2} \text{ (syst.) pb}$	$33.3^{+5.5}_{-5.3} \text{ (stat.)} {}^{+1.7}_{-1.3} \text{ (syst.) pb}$	$59.0^{+9.7}_{-9.2} \text{ (stat.)} {}^{+4.4}_{-3.5} \text{ (syst.) pb}$
SM predictions [7]	$19.2 \pm 0.9 \text{ pb}$	$24.5 \pm 1.1 \text{ pb}$	$55.5^{+2.4}_{-3.4} \text{ pb}$



Parameter	Best-fit value	SM prediction
$(\sigma \cdot B)_{ggF}^{ZZ} \text{ (pb)}$	$1.67 {}^{+0.41}_{-0.37}$	1.18 ± 0.07
$\sigma_{VBF}/\sigma_{ggF}$	$0.25 {}^{+0.15}_{-0.10}$	0.079 ± 0.004
$B^{\gamma\gamma}/B^{ZZ}$	$0.041 {}^{+0.015}_{-0.013}$	0.086 ± 0.003